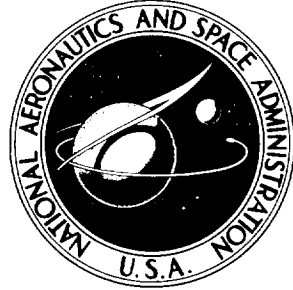NASA TECHNICAL NOTE

NASA TN D-7487

NASA TN D-7487

FORTRAN PROGRAM FOR PREDICTING OFF-DESIGN PERFORMANCE OF CENTRIFUGAL COMPRESSORS

by Michael R. Galvas

Lewis Research Center
and
U.S. Army Air Mobility R&D Laboratory
Cleveland, Ohio 44135

1. Report No. NASA TN D-7487	2. Government Accession No.	3. Recipient's Catalog No.
4. Title and Subtitle FORTRAN PROGRAM FOR PREDICTING OFF-DESIGN PERFORMANCE OF CENTRIFUGAL COMPRESSORS		5. Report Date November 1973
		6. Performing Organization Code
7. Author(s) Michael R. Galvas		8. Performing Organization Report No. E-7480
9. Performing Organization Name and Address NASA Lewis Research Center and U.S. Army Air Mobility R&D Laboratory Cleveland, Ohio 44135		10. Work Unit No. 501-24
		11. Contract or Grant No.
12. Sponsoring Agency Name and Address National Aeronautics and Space Administration Washington, D. C. 20546		13. Type of Report and Period Covered Technical Note
		14. Sponsoring Agency Code

15. Supplementary Notes

16. Abstract

A FORTRAN program for calculating the off-design performance of centrifugal compressors with channel diffusers is presented. Use of the program requires complete knowledge of the overall impeller and diffuser geometries. Individual losses are computed using analytical equations and empirical correlations which relate loss levels to velocity diagram characteristics and overall geometry. On a given speed line compressor performance is calculated for a range of inlet velocity levels. At flow rates between surge and choke, individual efficiency decrements, compressor overall efficiency, and compressor total pressure ratio are tabulated. An example case of performance comparison with a compressor built by a commercial engine manufacturer is presented to demonstrate the correlation with limited experimental data.

17. Key Words (Suggested by Author(s)) Centrifugal compressor Off-design performance		18. Distribution Statement Unclassified - unlimited		
19. Security Classif. (of this report) Unclassified	20. Security Classif. (of this page) Unclassified		21. No. of Pages 58	22. Price* Domestic, $3.50 Foreign, $6.00

FORTRAN PROGRAM FOR PREDICTING OFF-DESIGN PERFORMANCE

OF CENTRIFUGAL COMPRESSORS

by Michael R. Galvas

Lewis Research Center and
U. S. Army Air Mobility R&D Laboratory

SUMMARY

A FORTRAN program for calculating the off-design performance of centrifugal com-
pressors with channel diffusers is presented. Use of the program requires complete
knowledge of the overall impeller and diffuser geometries. Individual losses are com-
puted using analytical equations and empirical correlations which relate loss levels to
velocity diagram characteristics and overall geometry. On a given speed line com-
pressor performance is calculated for a range of inlet velocity levels. At flow rates
between surge and choke, individual efficiency decrements, compressor overall effi-
ciency, and compressor total pressure ratio are tabulated. An example case of per-
formance comparison with a compressor built by a commercial engine manufacturer is
presented to demonstrate the correlation with limited experimental data.

INTRODUCTION

Centrifugal compressors are frequently used in refrigeration cycles, refining sys-
tems, aircraft auxiliary systems, turboshaft engines, and other systems where light-
weight compact compression is required. The off-design performance characteristics
of centrifugal compressors are of interest because of the large effects that compressor
component performance has on overall cycle performance and because the compressor
is required to operate at off-design conditions much of the time. For turboshaft engines
assuming a drive turbine inlet temperature of 1422 K and efficiency of 90 percent, a
2.6-percent loss in compressor efficiency results in a 2-percent increase in engine
specific fuel consumption (SFC) and a 2.8-percent loss in engine power at design speed.
These losses become more pronounced at part-power settings. In addition to good per-
formance at off-design flow rates it is important that the compressor operate stably over

the range of flows and speeds required by the engine operating envelope. The usable range of the compressor pressure ratio-mass flow characteristic is bounded by the surge and choke mass flow rates. Operation at flows less than the surge point flow should be avoided because of potentially dangerous vibrations induced by the intermittent flow reversals and power loss. Operation with the compressor choked is generally avoided because of the poor compressor efficiency and pressure ratio at the choke point. The problem undertaken in this analysis is to determine the centrifugal compressor performance characteristics over a range of rotative speeds and flow rates and predict the usable range of flow rates at which the compressor can operate. The method of analysis uses the loss correlations and equations of reference 1 with surge and choke criteria added to predict compressor operating range.

A FORTRAN program has been developed at NASA Lewis Research Center which predicts centrifugal compressor performance through utilization of empirical correlations which are related to the compressor geometry and velocity diagram characteristics. A complete knowledge of the compressor overall geometry and working fluid inlet total conditions is required for its use. Working fluid state conditions and flow properties are calculated using a mean streamline one-dimensional analysis. The program is limited to centrifugal compressors with channel diffusers operating up to their choke point. A comparison of calculated and experimental performance is given to demonstrate the correlation with limited experimental data. The experimental data presented for comparison were obtained from a compressor developed by Solar Aircraft Company, Division of International Harvester, Inc. Shock losses in the rotor are neglected. Clearance losses are considered to be inherent in the impeller losses since good performance correlation is achieved on compressors operating with reasonable clearances.

METHOD OF ANALYSIS

Input values of $(V/V_{cr})_0$ are used to determine compressor mass flow rate. (Symbols are defined in appendix A and compressor stations are shown in fig. 1.) Individual losses are calculated using velocity diagram characteristics and empirical correlations determined by the input absolute velocity level and compressor geometry. For compressors having inlet guide vanes it is assumed that the vanes are placed in a constant-area annulus having no wall curvatures or slopes. Overall compressor efficiency, total pressure ratio, and mass flow rate are tabulated for each operating point inside the predicted range for each speed line that is input. A complete discussion of the loss calculations is discussed in appendix B.
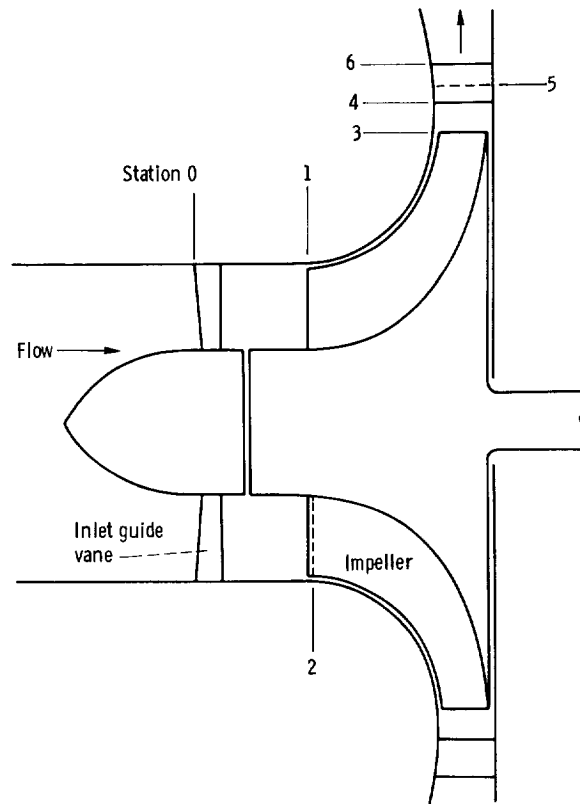
2

Figure 1. - Meridional cross section of compressor.

Required Information

The compressor data needed to use the FORTRAN program are the following:
inducer inlet tip diameter, inducer inlet hub-tip diameter ratio, inducer inlet blade angle
at the root-mean-square diameter, inducer blade blockage at the rms diameter, inducer
inlet hub and tip wall slopes, inducer inlet hub and tip wall curvatures, inlet solid-body
swirl angle at the rms diameter, inducer-tip to impeller-exit diameter ratio, impeller
exit blade angle, impeller blade exit height, number of impeller blades at exit, vaneless
diffuser diameter ratio, vaned diffuser setting angle, total vaned diffuser throat area,
vaned diffuser area ratio, skin friction coefficient of the wetted surfaces, design rotative
speed, and the fraction of design rotative speed for which the calculations are to be per-
formed.

The working fluid properties and state conditions required are: inlet total pressure,
inlet total temperature, inlet dynamic viscosity based on total conditions, specific heat
ratio, and gas constant.

Two control variables are used to select the options of solid-body prewhirl and im-
pellers with splitter blades. Inducer inlet hub and tip wall slopes and curvatures are all

3

set equal to zero for compressors with inlet guide vanes.

Information which corresponds to the design speed line for the example compressor is as follows:

Compressor data
Design rotative speed, N, rpm 72 000
Inducer inlet tip diameter, D_{1T}, m 0.0813
Inducer hub-tip diameter ratio, λ 0.5313
Inducer inlet hub wall curvature, C_{1H}, m^{-1} (positive around axis of rotation) 0
Inducer inlet tip wall curvature, C_{1T}, m^{-1} (positive around axis of rotation) 0
Inducer inlet hub wall slope, χ_H, deg from axial 7
Inducer inlet tip wall slope, χ_T, deg from axial 0
Inducer inlet blade angle at the rms diameter, β_{1MFb}, deg from meridional 49.0
Inducer-tip to impeller-exit diameter ratio, D_{1T}/D_3 . . . . 0.5614
Number of impeller blades at exit, Z_3 32
Impeller blade exit angle, β_3, deg from meridional (positive opposite to direction of rotation) 25
Impeller exit blade height, b_3, m 0.0051
Vaneless diffuser diameter ratio, D_4/D_3 . . . . 1.14
Vaned diffuser setting angle, α_4, deg from meridional 78
Total vaned diffuser throat area, A_5, m^2 . . . . 0.00071
Vaned diffuser area ratio, A_6/A_5 . . . . 2.7
Friction coefficient, C_f 0.004

Working fluid properties and state conditions
Specific heat ratio, γ 1.4
Gas constant, R, J/(kg)(K) 287.05
Inlet total pressure, p_0', N/m^2 . . . . 101 325
Inlet total temperature, T_0', K 288.15
Inlet dynamic viscosity based on total conditions, μ_0', $N\text{-}sec/m^2$ . . . . 1.788×10^{-5}

Velocity diagram properties
Number of values of compressor inlet absolute critical velocity ratios used in calculating performance . . 15
Compressor inlet absolute critical velocity ratios, $\left(V/V_{cr}\right)_0$ . . . . 0.47 to 0.61
Inducer inlet solid-body swirl angle at the rms diameter, α_{1MF}, deg from meridional 0
Splitter control variable, SPLT (SPLT = 0, no splitter blades; SPLT = 1, splitters) 1

Calculated Losses

Inlet guide vane loss. - Equations relating working fluid kinetic energy level, boundary layer, and blade geometry were developed for axial turbine stators in reference 2. These equations were used to calculate state conditions downstream of the inlet guide vanes; thus the velocity diagram characteristics were found by satisfying one-dimensional continuity.

An inlet guide vane loss coefficient is calculated using the same assumptions about blade geometry and boundary layer characteristics as used in reference 3. The inlet guide vane loss is then calculated as a fraction of the ideal kinetic energy at the rms diameter.

Inducer incidence loss. - Reference 4 developed equations for optimum inducer incidence angle of centrifugal compressors with axial inlets. The optimum incidence angle is calculated from the inlet velocity diagram characteristics and blade blockage at the rms diameter assuming an incompressible working fluid. The enthalpy loss due to incidence is calculated assuming that the relative velocity component normal to the optimum incidence angle is lost. Therefore, the incidence loss is simply

$$\Delta h_{INC} = \frac{W_L^2}{2C_p}$$

where

$$W_L = W_{1MF} \sin \left| \beta_{opt} - \beta_{1MF} \right|$$

Blade loading loss. - Boundary layer growth in the impeller is highly dependent on the diffusion of the working fluid internal to the impeller itself. Reference 5 proposed an equation for calculating the diffusion factor of the impeller based on a uniform velocity loading along the blade chord. This equation is used to calculate the impeller diffusion factor for impellers without splitters. A modified form, with reduced penalty due to aerodynamic work input, is used for impellers which have a set of splitter blades. With the diffusion factor calculated by these methods the blade loading loss was expressed as

$$\Delta h_{BL} = 0.05 \, D_f^2 u_3^2$$

Skin friction loss. - In addition to the losses resulting from the aerodynamic loading of the impeller blades, the impeller incurs losses due to skin friction of the impeller

and shroud wetted areas. Reference 5 developed an equation for this loss based on fully developed turbulent pipe flow. In the case of impellers with splitter blade rows, the empirical constant appearing in the equation is modified to account for the higher mean channel relative velocity caused by the addition of splitters. The general equation used for skin friction loss is

$$\Delta h_{SF} = K_{DF} C_f \frac{\dfrac{L}{D_3}}{\dfrac{D_{HYD}}{D_3}} \left(\frac{w}{u_3}\right)^2_{av} u_3^2$$

where $K_{SF} = 5.6$ for conventional impellers and $K_{SF} = 7.0$ for impellers with tandem blades.

Disk friction loss. - The specific loss due to windage on the compressor back face is calculated using the equation

$$\Delta h_{DF} = 0.01356 \frac{\rho_3}{w \, Re^{0.2}} u_3^3 D_3^2$$

This is a form of the disk friction power loss of reference 6.

Recirculation loss. - Losses resulting from work done on the working fluid due to backflow into the impeller are expressed as

$$\Delta h_{RC} = 0.02 \sqrt{\tan \alpha_3} \, D_f^2 u_3^2$$

This is a modification of the equation proposed in reference 5.

Vaneless diffuser loss. - The flow angle and Mach number variation with radius in the vaneless space are determined by numerical solution of the differential equations for vaneless space flow developed in reference 7. The equations are simplified through the assumptions of adiabatic flow and constant geometric depth passage. The radial total pressure distribution in the vaneless space is calculated using the equation derived in reference 5. When the fluid state and flow properties are determined at the vaned diffuser leading edge radius by the methods described previously, the vaneless diffuser loss is calculated from the equation

6

$$\Delta h_{VLD} = C_p T_3' \left[\left(\frac{p_4}{p_4'} \right)^{(\gamma-1)/\gamma} - \left(\frac{p_4}{p_3'} \right)^{(\gamma-1)/\gamma} \right]$$

Vaned diffuser loss. - Curves of maximum static pressure recovery coefficient at a given area ratio were extrapolated from the test data for square throat diffusers reported in reference 8 for various combinations of vaned diffuser throat Mach number, aerodynamic blockage, and area ratio. These data were recorded for channel diffusers with symmetrical pressure loadings about the channel centerline. The vaned diffuser in a centrifugal compressor is loaded with a pressure gradient across the channel. In this analysis it was assumed that the difference in the loadings between the test diffusers of reference 8 and the compressor diffusers would have no effect on calculated diffuser recovery. A one-seventh power velocity distribution in the boundary layer along the vaneless space endwalls is used to calculate the displacement thickness representing vaned diffuser throat blockage. The value of static pressure recovery coefficient C_p^{**} corresponding to the vaned diffuser geometric area ratio, inlet Mach number, and aerodynamic blockage is extrapolated from the test data.

The vaned diffuser exit critical velocity ratio is calculated using one-dimensional continuity. Vaned diffuser loss is then calculated using the equation

$$\Delta h_{VD} = C_p T_3' \left[\left(\frac{p_6}{p_6'} \right)^{(\gamma-1)/\gamma} - \left(\frac{p_6}{p_5'} \right)^{(\gamma-1)/\gamma} \right]$$

Calculation of Compressor Choking Flow

Two criteria are used in the prediction of compressor choking flow: (1) inducer choke and (2) vaned diffuser choke. Reference 9 presented data on inducer choking incidence levels as functions of relative Mach number and blade angle at the rms diameter for inducer pitch-chord ratios of 0.5 and thickness-chord ratios of 0.05. These data were used to predict compressor choking flow due to inducer choke.

Vaned diffuser choke is predicted from one-dimensional continuity using the computed values of weight flow, total temperature, total pressure, aerodynamic blockage, and the geometric throat area. The maximum value of the one-dimensional weight flow function is calculated from the equation

7

$$\left(\frac{w\sqrt{T_3'}}{p_5'A_5B_5}\right)_{max} = \sqrt{\frac{\gamma}{R}\left(\frac{2}{\gamma+1}\right)^{(\gamma+1)/(\gamma-1)}}$$

At the first input critical velocity ratio where the left side of the equation equals or exceeds the right side the compressor is choked. One would expect the speed lines to have infinite slopes at the choke point. The vertical portions of the speed lines are approximated through the assumption of zero static pressure recovery in the vaned diffuser for the cases of vaned diffuser choke. The impeller characteristic should exhibit a vertical slope at the impeller choke point but this is not predicted by the correlations used.

Calculation of Compressor Surge Point

The vaned diffuser is assumed to be the component which governs the location of the compressor surge point. Examination of performance characteristics of centrifugal compressors covering a range of pressure ratios indicates that compressor flow range can be expressed as a function of the vaned diffuser leading edge Mach number. With a good impeller-diffuser throat area match the flow range will vary with the diffuser leading edge Mach number as shown in figure 2. This curve was deduced from unpublished operating range data for centrifugal compressors with design point pressure ratios ranging from 1.9 to 10.0.
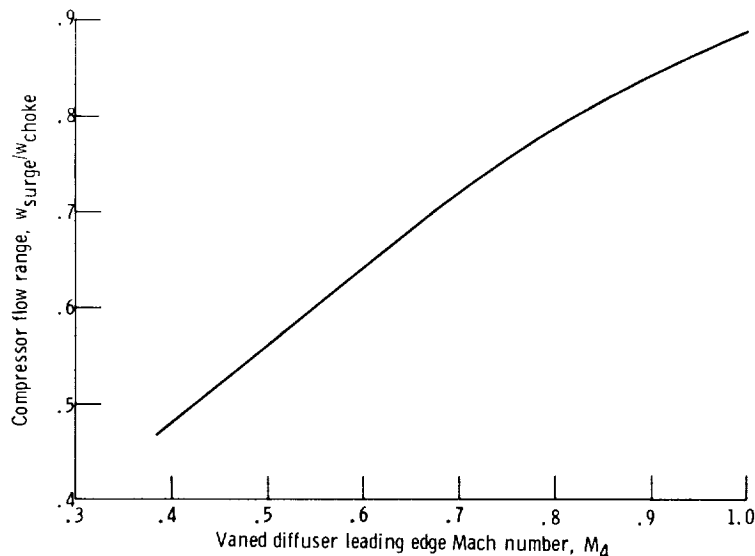

Figure 2. - Compressor flow range as a function of vaned diffuser leading edge Mach number.

8

Comparison of Estimated and Experimental Performance

This section compares the results obtained by the analytical procedure described herein to the experimental results obtained with a commercially manufactured centrifugal compressor.

Figure 3 shows the comparison between calculated and experimental pressure ratios as functions of corrected flow for 60, 80, 90, and 100 percent rotative speeds. Choking flow is caused by inducer choke at 100 percent speed and by diffuser choke at the other speeds. The assumption of zero static pressure recovery at the vaned diffuser choke point permits an estimate of the flow rate at which the compressor pressure ratio characteristic becomes vertical. Experimentally, the impeller characteristic exhibits behavior similar to that of the diffuser at the choked condition. However, the multidimensional effects that characterize this behavior apparently cannot be approximated accurately with strictly one-dimensional correlations. Modifying the correlations for evaluation at the hub, mean, and tip sections and averaging the results may help to predict the gradual pressure ratio reduction in moving toward choke. The potential refinements offered by this approach have not yet been considered herein. Maximum error in predicting the choking weight flow occurs at the 90 percent speed line and is 25 percent. Maximum error in predicting the compressor operating range (w_{surge}/w_{choke}) occurs at the 80 percent speed line and is 8.1 percent.

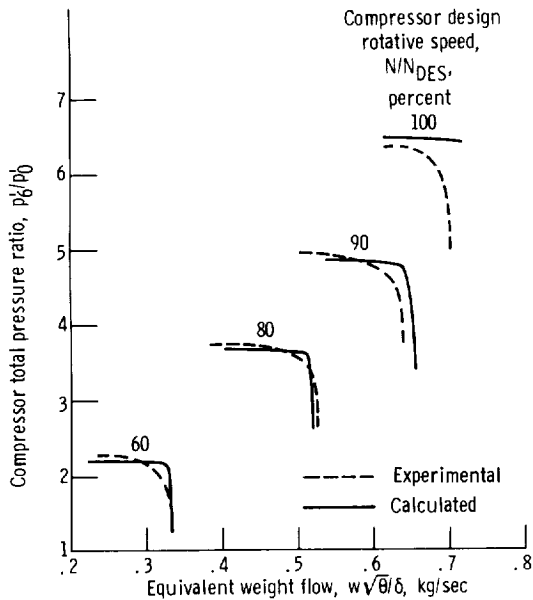Figure 4 shows the comparison between calculated and experimental efficiencies as

Figure 3. – Comparison of calculated and experimental compressor total pressure ratios as functions of equivalent weight flow and rotative speeds.
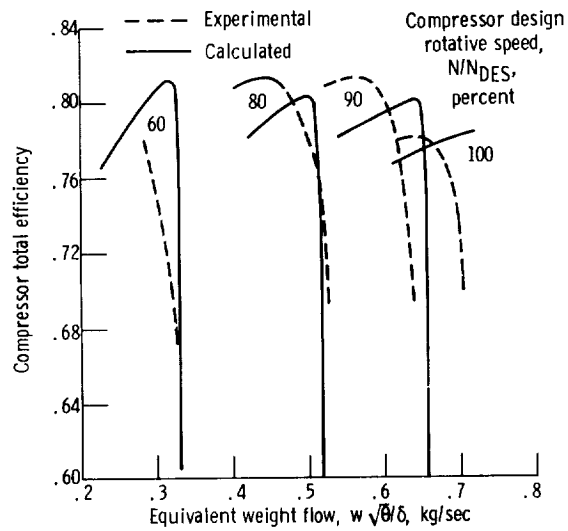
Figure 4. – Comparison of calculated and experimental compressor total efficiencies as functions of equivalent weight flow and rotative speeds.

functions of corrected flow. The worst estimate of peak efficiency occurs at the 90 percent speed line and is in error by 1.2 points. Only partial data is shown for the efficiency contour at 60 percent speed. This results because the data is replotted from a performance map that had efficiency contours and more data could not be accurately interpolated. Predicted surge point efficiencies for all speed lines are considerably lower than those experimentally measured. This can be attributed to predicted diffuser pressure recovery being lower than that attainable experimentally. Aerodynamic blockage growth may not be as rapid as that predicted by the model in moving toward surge.

Compressor efficiency increases with increasing flow until the choke point is reached. At the choke point vaned diffuser static pressure recovery decreases, resulting in a decrease in overall compressor efficiency. At the impeller choke point one would expect the impeller losses to increase substantially, resulting in a decrease in overall compressor efficiency. However, this behavior is not predicted through the use of the empirical correlations.

CONCLUDING REMARKS

This section summarizes the pertinent characteristics of the prediction method, discusses the limitations of the method, and notes the effect of the limitations on the results.

For inducers with relative Mach numbers appreciably in excess of unity the predicted compressor total pressure ratio and efficiency are greater than that attainable experimentally. This is a result of neglecting shock losses in the inducer inlet.

Predicted static pressure recovery for vaned diffusers with throat Mach numbers greater than unity will be too large. Extrapolation of the channel diffuser data used in the program is valid only in the subsonic flow regime.

The prewhirl option available in the program is for solid-body vortex swirl. This type of swirl is used primarily because it minimizes inducer inlet tip relative Mach number.

Compressor total pressure ratio and efficiency are not adequately predicted with the one-dimensional correlations when the compressor mass flow rate is limited by the impeller rather than the vaned diffuser. The predicted total pressure ratio and efficiency levels are higher than those measured experimentally.

Predicted surge point efficiencies are considerably lower than those measured on the example compressor. Correlation with experimental data from other compressors indicates that the predicted surge point efficiencies are sometimes higher and sometimes lower than the corresponding experimental values. This may be due in part to the difficulty encountered in making precise measurements at this flow condition.

10

FORTRAN PROGRAM

Program Input

The information required for the program is input using NAMELIST format. A sample input sheet, with the data used for generating the 100 percent speed line for the example compressor, is shown in figure 5. The definitions of the FORTRAN input variables are:

ADTH   total vaned diffuser throat area, A_5, m^2

AL1MF   inducer inlet absolute flow angle for solid-body swirl at rms diameter, α_{1MF}

AL3   vaned diffuser setting angle, α_4, deg from meridional

AR   vaned diffuser area ratio, A_6/A_5

B1MFB   inducer rms blade angle, β_{1MFb}, deg from meridional

B2   impeller exit blade height, b_3, m

B2X   impeller blade exit backsweep, β_{3b}, deg from meridional

BLOCK   inducer rms blade blockage function

Figure 5. - Sample input sheet.

CF	skin friction coefficient, C_f
CHIH	inducer inlet hub wall slope, χ_{1H}, deg from axial
CHIT	inducer inlet tip wall slope, χ_{1T}, deg from axial
CURVH	inducer inlet hub curvature, C_{1H}, m^{-1}
CURVT	inducer inlet tip curvature, C_{1T}, m^{-1}
DRAT	inducer-tip to impeller-exit diameter ratio, D_{1T}/D_3
DIT	inducer tip diameter, D_{1T}, m
GAM	specific heat ratio, γ
LAMX	inducer hub-tip diameter ratio, λ
MU0	total inlet dynamic viscosity, μ_0', N-sec/m^2
N	compressor design rotative speed, N_{DES}, rpm
NONDES	percent compressor design rotative speed, N/N_{DES}
NVOVCR	number of input values of $(V/V_{cr})_0$
POP	total inlet pressure, p_0', N/m^2
RGAS	gas constant, R, J/(kg)(K)
SPLT	control variable for splitter calculations (SPLT = 0, conventional impeller; SPLT = 1, impeller with splitters)
TOP	inlet total temperature, T_0', K
VLDRR	vaneless diffuser diameter ratio, D_4/D_3
VOVCR	values of inlet critical velocity ratio, $(V/V_{cr})_0$
Z	number of impeller blades at exit, Z_3

Sample Output

In the normal mode of operation the program performs two iterations over the range of inlet absolute critical velocity ratios which are specified. On the first iteration the compressor choking flow rate is determined. On the second iteration the printout of compressor performance at flow rates outside the usable range is deleted. A listing of the input information is tabulated for the compressor configuration studied. Then the compressor surge and choke flow rates are printed out. Finally, for each calculated point inside the operating range, compressor equivalent weight flow, total pressure ratio, total efficiency, and individual efficiency decrements are printed out. Sample output for the example compressor is as follows:

12

INLET TOTAL PRESSURE 101325.
INLET TOTAL TEMPERATURE 288.15
INLET TOTAL DYNAMIC VISCOSITY .0000179
SPECIFIC HEAT RATIO 1.4
GAS CONSTANT 287.05

NUMBER OF BLADES 32.
FRICTION COEFFICIENT .004
SPLIT 1
DESIGN SPEED 72000.
INDUCER RMS SWIRL ANGLE 0.
INDUCER RMS BLOCKAGE FACTOR 0.90

INDUCER RMS BLADE ANGLE 49.0
INDUCER HUB-TIP DIAMETER RATIO 0.5313
INDUCER TIP-IMPELLER EXIT DIAMETER RATIO 0.5614

IMPELLER BLADE EXIT BACKSWEEP 25.0
IMPELLER BLADE EXIT HT. .03510
VANELESS DIFFUSER DIAMETER RATIO 1.140
VANED DIFFUSER SETTING ANGLE 78.00
TOTAL VANED DIFFUSER THROAT AREA .000710
VANED DIFFUSER AREA RATIO 2.70

INLET CRITICAL VELOCITY RATIO ARRAY

0.47	0.48	0.49	0.50	0.51	0.52	0.53	0.54
0.55	0.56	0.57	0.58	0.59	0.60	0.61	

AT FLOW LESS THAN SURGE FOR V/VCR=0.47

PERCENT NDES 100.0
SURGE FLOW RATE 0.614
CHOKE FLOW RATE 0.719

DETAIGV	DETAINC	DETABL	DETASF	DETARC	DETADF	DETAVLD	DETAVD	WEQ	PRESSURE RATIO	ETAT
.	.00035	.03264	.05138	.02885	.03603	.02651	.05619	0.616	6.485	.768
.	.00037	.03233	.05199	.02828	.03546	.02604	.05511	0.626	6.485	.770
.	.00038	.03205	.05259	.02776	.03494	.02561	.05412	0.636	6.484	.773
.	.00039	.03177	.05321	.02726	.03444	.02520	.05322	0.646	6.481	.775
.	.00040	.03150	.05384	.02678	.03397	.02481	.05239	0.656	6.477	.776
.	.00041	.03123	.05448	.02632	.03351	.02443	.05163	0.665	6.472	.778
.	.00042	.03097	.05513	.02587	.03307	.02407	.05096	0.675	6.465	.780
.	.00043	.03072	.05579	.02544	.03264	.02372	.05036	0.684	6.458	.781
.	.00044	.03047	.05647	.02503	.03224	.02338	.04983	0.693	6.448	.782
.	.00045	.03024	.05716	.02463	.03184	.02306	.04938	0.702	6.438	.783
.	.00046	.03000	.05785	.02425	.03147	.02275	.04930	0.710	6.427	.784
.	.00047	.02978	.05856	.02388	.03111	.02245	.04870	0.719	6.414	.785

13

INLET TOTAL PRESSURE 101325.
INLET TOTAL TEMPERATURE 288.15
INLET TOTAL DYNAMIC VISCOSITY .0000179
SPECIFIC HEAT RATIO 1.4
GAS CONSTANT 287.05

NUMBER OF BLADES 32.
FRICTION COEFFICIENT .004
SPLT 1
DESIGN SPEED 72000.
INDUCER RMS SWIRL ANGLE 0.
INDUCER RMS BLOCKAGE FACTOR 0.90

INDUCER RMS BLADE ANGLE 49.0
INDUCER HUB-TIP DIAMETER RATIO 0.5313
INDUCER TIP-IMPELLER EXIT DIAMETER RATIO 0.5614

IMPELLER BLADE EXIT BACKSWEEP 25.0
IMPELLER BLADE EXIT HT. .03510
VANELESS DIFFUSER DIAMETER RATIO 1.140
VANED DIFFUSER DIAMETER RATIO 0.5614
VANED DIFFUSER SETTING ANGLE 78.00

TOTAL VANED DIFFUSER THROAT AREA .000710
TOTAL VANED DIFFUSER AREA RATIO 2.70

INLET CRITICAL VELOCITY RATIO ARRAY

| 0.39 | 0.40 | 0.41 | 0.42 | 0.43 | 0.44 | 0.45 | 0.46 |
| 0.47 | 0.48 | 0.49 | 0.50 | 0.51 | 0.52 | 0.53 | |

AT FLOW LESS THAN SURGE FOR W/VCR=0.39
AT FLOW LESS THAN SURGE FOR W/VCR=0.40

PERCENT NDES 90.0
SURGE FLOW RATE 0.540
CHOKE FLOW RATE 0.656

DETAIGV	DETAINC	WEO	DETABL	PRESSURE RATIO	DETASF	DETADF	ETAT	DETARC	DETAVLD	DETAVD
.	.00034	0.540	.02969	4.857	.05390	.03316	.782	.02450	.02334	.05277
.	.00035	0.552	.02926	4.863	.05468	.03254	.786	.02384	.02285	.05027
.	.00036	0.563	.02883	4.846	.05548	.03195	.787	.02321	.02238	.05074
.	.00037	0.574	.02841	4.849	.05630	.03139	.791	.02260	.02193	.04834
.	.00039	0.584	.02800	4.831	.05715	.03086	.791	.02201	.02151	.04881
.	.00040	0.595	.02759	4.833	.05801	.03034	.795	.02144	.02110	.04651
.	.00041	0.605	.02720	4.814	.05890	.02985	.795	.02090	.02071	.04698
.	.00043	0.616	.02681	4.814	.05980	.02938	.798	.02038	.02034	.04479
.	.00044	0.626	.02643	4.794	.06073	.02893	.798	.01988	.01999	.04525
.	.00045	0.636	.02606	4.792	.06167	.02849	.801	.01939	.01965	.04316
.	.00046	0.646	.02570	4.789	.06264	.02808	.804	.01893	.01932	.04114
.	.00048	0.656	.02535	3.381	.06363	.02768	.591	.01848	.01901	.25445

14

INLET TOTAL PRESSURE INLET TOTAL TEMPERATURE INLET TOTAL DYNAMIC VISCOSITY SPECIFIC HEAT RATIO GAS CONSTANT
101325.   288.15   .0000179   1.4   287.05

NUMBER OF BLADES FRICTION COEFFICIENT SPLT DESIGN SPEED INDUCER RMS SWIRL ANGLE INDUCER RMS BLOCKAGE FACTOR
32.   .004   1   72000.   0.   0.90

INDUCER RMS BLADE ANGLE INDUCER HUB-TIP DIAMETER RATIO INDUCER TIP-IMPELLER EXIT DIAMETER RATIO
49.0   0.5313   0.5614

IMPELLER BLADE EXIT BACKSWEEP IMPELLER BLADE EXIT HT. VANELESS DIFFUSER DIAMETER RATIO VANED DIFFUSER SETTING ANGLE
25.0   .00510   1.140   78.00

TOTAL VANED DIFFUSER THROAT AREA   VANED DIFFUSER AREA RATIO
.003710   2.70

INLET CRITICAL VELOCITY RATIO ARRAY
0.27   0.28   0.29   0.30
0.35   0.36   0.37   0.38
0.31   0.32   0.33   0.34
0.39   0.40   0.41

WT FLOW LESS THAN SURGE FOR V/VCR=0.27
WT FLOW LESS THAN SURGE FOR V/VCR=0.28
WT FLOW LESS THAN SURGE FOR V/VCR=0.29
WT FLOW LESS THAN SURGE FOR V/VCR=0.30

PERCENT NDES

SURGE FLOW RATE   CHOKE FLOW RATE
0.409   0.518

PERCENT NDES 80.0

Parameter									
WEQ	0.421	0.434	0.446	0.458	0.470	0.482	0.494	0.506	0.518
PRESSURE RATIO	3.677	3.676	3.676	3.674	3.672	3.654	3.651	3.648	2.717
ETAT	.781	.786	.790	.794	.798	.799	.802	.806	.596
DETABL	.02912	.02845	.02780	.02717	.02654	.02592	.02532	.02472	.02414
DETAINC	-.00026	-.00028	-.00029	-.00031	-.00032	-.00034	-.00035	-.00037	-.00038
DETASF	.05321	.05416	.05512	.05611	.05714	.05821	.05932	.06046	.06164
DETADF	.03395	.03306	.03225	.03148	.03075	.03006	.02941	.02879	.02820
DETARC	.02404	.02307	.02217	.02131	.02048	.01970	.01895	.01823	.01754
DETAVLD	.02311	.02243	.02180	.02121	.02365	.02013	.01963	.01916	.01872
DETAVD	.05537	.05289	.05070	.04848	.04623	.04705	.04466	.04224	.25375
DETAIGV	0.	0.	0.	0.	0.	0.	0.	0.	0.

15

INLET TOTAL PRESSURE   INLET TOTAL TEMPERATURE   INLET TOTAL DYNAMIC VISCOSITY   SPECIFIC HEAT RATIO   GAS CONSTANT
101325.   288.15   .0000179   1.4   287.05

NUMBER OF BLADES   FRICTION COEFFICIENT   SPLT   DESIGN SPEED   INDUCER RMS SWIRL ANGLE   INDUCER RMS BLOCKAGE FACTOR
32.   .004   1   7200.   0.   0.90

INDUCER RMS BLADE ANGLE   INDUCER HUB-TIP DIAMETER RATIO   INDUCER TIP-IMPELLER EXIT DIAMETER RATIO
49.0   0.5513   0.5614

IMPELLER BLADE EXIT BACKSWEEP   IMPELLER BLADE EXIT HT.   VANELESS DIFFUSER DIAMETER RATIO   VANED DIFFUSER SETTING ANGLE
25.0   .00510   1.140   78.00

TOTAL VANED DIFFUSER THROAT AREA   VANED DIFFUSER AREA RATIO
.000710   2.70

INLET CRITICAL VELOCITY RATIO ARRAY

0.15	0.16	0.17	0.18
0.23	0.24	0.25	0.26
0.19	0.20	0.21	0.22

AT FLOW LESS THAN SURGE FOR V/VCR=0.15

PERCENT NDES

SURGE FLOW RATE   CHOKE FLOW RATE
0.223   0.331

WEQ	PRESSURE RATIO	DETADF	ETAT
0.224	2.209	.03944	.766

DETAIGV	DETAINC	DETABL	DETASF	DETARC	DETAVLD	DETAVD
.	.00014	.03086	.05113	.02711	.02516	.05969

WEQ	PRESSURE RATIO	DETADF	ETAT
0.238	2.209	.03750	.775

DETAIGV	DETAINC	DETABL	DETASF	DETARC	DETAVLD	DETAVD
.	.00016	.02958	.05236	.02513	.02377	.05682

WEQ	PRESSURE RATIO	DETADF	ETAT
0.251	2.198	.03576	.777

DETAIGV	DETAINC	DETABL	DETASF	DETARC	DETAVLD	DETAVD
.	.00017	.02831	.05369	.02331	.02253	.05939

WEQ	PRESSURE RATIO	DETADF	ETAT
0.265	2.198	.03420	.785

DETAIGV	DETAINC	DETABL	DETASF	DETARC	DETAVLD	DETAVD
.	.00019	.02706	.05510	.02161	.02142	.05543

WEQ	PRESSURE RATIO	DETADF	ETAT
0.278	2.199	.03278	.793

DETAIGV	DETAINC	DETABL	DETASF	DETARC	DETAVLD	DETAVD
.	.00021	.02583	.05661	.02004	.02041	.05108

WEQ	PRESSURE RATIO	DETADF	ETAT
0.292	2.199	.03148	.801

DETAIGV	DETAINC	DETABL	DETASF	DETARC	DETAVLD	DETAVD
.	.00023	.02462	.05822	.01857	.01950	.04634

WEQ	PRESSURE RATIO	DETADF	ETAT
0.305	2.199	.03030	.809

DETAIGV	DETAINC	DETABL	DETASF	DETARC	DETAVLD	DETAVD
.	.00025	.02343	.05993	.01721	.01868	.04120

WEQ	PRESSURE RATIO	DETADF	ETAT
0.318	2.198	.02919	.817

DETAIGV	DETAINC	DETABL	DETASF	DETARC	DETAVLD	DETAVD
.	.00027	.02224	.06179	.01590	.01791	.03559

WEQ	PRESSURE RATIO	DETADF	ETAT
0.331	1.814	.02819	.606

DETAIGV	DETAINC	DETABL	DETASF	DETARC	DETAVLD	DETAVD
.	.00029	.02109	.06372	.01471	.01722	.24910

REC= 00000 FIL= 00002

Definitions of the abbreviated FORTRAN output variables are:

DETABL	efficiency decrement due to impeller blade aerodynamic loading, $\Delta\eta_{BL}$
DETADF	efficiency decrement due to disk friction, $\Delta\eta_{DF}$
DETAIGV	efficiency decrement due to inlet guide vane loss, $\Delta\eta_{IGV}$
DETAINC	efficiency decrement due to inducer incidence, $\Delta\eta_{INC}$
DETARC	efficiency decrement due to recirculation, $\Delta\eta_{RC}$
DETASF	efficiency decrement due to skin friction, $\Delta\eta_{SF}$
DETAVD	efficiency decrement due to vaned diffuser losses, $\Delta\eta_{VD}$
DETAVLD	efficiency decrement due to vaneless diffuser losses, $\Delta\eta_{VLD}$
ETAT	compressor total efficiency, η
WEQ	equivalent flow rate, $w\sqrt{\theta}/\delta$, kg/sec

Error Messages

If the compressor choking flow rate is not reached with the specified values of inlet absolute critical velocity ratios, the operating range cannot be determined with the methods used in this analysis. When this happens, the calculated performance output is deleted and the message COMPRESSOR CHOKING FLOW HAS NOT BEEN REACHED is printed.

If the first input value of $\left(V/V_{cr}\right)_0$ results in calculated weight flow greater than the compressor choking weight flow, the message VOVCR ARRAY TOO LARGE is printed.

For input values of $\left(V/V_{cr}\right)_0$ much too small for the compressor of interest a velocity diagram solution at the impeller exit cannot be obtained. When this occurs the message IRRATIONAL EXIT TRIANGLE is printed. All of these problems can be corrected by making the appropriate adjustments to the VOVCR array used.

Main Program FORTRAN Variables and Corresponding Engineering Symbols

A1	a_1
A2	a_3
ACOUSR	a/a'

ADTH	A_5
AL1	α_{1T}
AL1MF	α_{1MF}
AL2	α_3
AL3	α_4
ALPH1	temporary storage
ALPHA	α
AMT	M_5
AMU	μ
AMULT	$\exp\left(\int_{r_{1H}}^{r_{1MF}} C\,dn\right)$
ANU	ν
AR	A_6/A_5
B	B_5
B0	B_0
B1	β_{1T}
B1H	β_{1H}
B1MF	β_{1MF}
B1MFB	β_{1MFb}
B2	b_3
B2X	β_{3b}
BARR	array of vaned diffuser throat blockages
BLOCK	B_1
BMULT	$\exp\left(\int_{r_{1MF}}^{r_{1T}} C\,dn\right)$
BOPT	β_{1MFopt}
BT	vaned diffuser inlet blockage
CF	C_f

18

CHIH	χ_{1H}
CHIMF	χ_{1MF}
CHIT	χ_{1T}
CINC	inducer choking incidence
CINC1	interpolation variable
CINC2	interpolation variable
CINC40	choking incidence array for 40° rms inducer blade angles
CINC50	choking incidence array for 50° rms inducer blade angles
CINC60	choking incidence array for 60° rms inducer blade angles
CONST1	K_{BL}
CONST2	K_{SF}
COSA	$\cos \alpha_{1T}$
CP	C_p
CPSTAR	C_p^{**}
CURVH	C_{1H}
CURVMF	C_{1MF}
CURVT	C_{1T}
D1H	D_{1H}
D1T	D_{1T}
D2	D_3
DEBL	$\Delta\eta_{BL}$
DEDF	$\Delta\eta_{DF}$
DEEXIT	$\Delta\eta_{exit}$
DEIGV	$\Delta\eta_{IGV}$
DEINC	$\Delta\eta_{INC}$
DELTA	δ
DELTAB	ΔB
DELTAR	Δr
DELTAS	$\Delta\delta^*$

DERC	$\Delta\eta_{RC}$
DESF	$\Delta\eta_{SF}$
DEVD	$\Delta\eta_{VD}$
DEVLD	$\Delta\eta_{VLD}$
DF	D_f
DHACT	Δh_{act}
DHAERO	Δh_{aero}
DHBL	Δh_{BL}
DHDF	Δh_{DF}
DHDIF	Δh_{VD}
DHEST	Δh_{est}
DHIGV	Δh_{IGV}
DHINC	Δh_{INC}
DHRC	Δh_{RC}
DHSF	Δh_{SF}
DHVLD	Δh_{VLD}
DHYD	D_{HYD}/D_3
DIFLEM	M_4 array
DMF	D_{1MF}
DRAT	D_{1T}/D_3
EPS	ϵ
ETAD	η_{AD}
ETAR	η_R
EWF	$w\sqrt{\theta}/\delta$
F1	C_p^{**} at vaned diffuser area ratio of 1.2
F2	C_p^{**} at vaned diffuser area ratio of 2.0
F3	C_p^{**} at vaned diffuser area ratio of 3.0
F4	C_p^{**} at vaned diffuser area ratio of 4.0
F5	C_p^{**} at vaned diffuser area ratio of 5.0

FINT	$\displaystyle\int_{r_{1H}}^{r_{1MF}} C\,dn$
FLFUNC	$\displaystyle\sqrt{\frac{\gamma}{R}\left(\frac{2}{\gamma+1}\right)^{(\gamma+1)/(\gamma-1)}}$
FLRNG	w_{surge}/w_{choke}
G1	$\gamma+1$
G2	$\gamma-1$
GAM	γ
GINT	$\displaystyle\int_{r_{1H}}^{r_{1T}} C\,dn$
H0	$r_{1MF}-r_{1H}$
H1	$r_{1T}-r_{1MF}$
HIS	Δh_{is}
INC	$\beta_{1MF}-\beta_{1MFb}$
J	index variable
JAN	iteration counter
K	choke indication variable
L	index variable
LAMX	λ
LOD	L/D_3
MIN	index variable
MU0	μ_0'
MWRMS	array of inducer rms relative Mach numbers
N	N_{DES}
NO	index variable
NONDES	N/N_{DES}
NVOVCR	number of values of $\left(V/V_{cr}\right)_0$
NWRITE	output control variable

POP	p_0'
P1	p_{1MF}
P1P	p_{1MF}'
P2	p_3
P2P	p_3'
P3P	p_4'
P4	p_6
P4PG	iteration variable
P4PL	iteration variable
PEXIT	p_6
PHI	φ
PIMF	p_{2MF}
PIPMF	p_{2MF}'
POPP1	$(p/p')_{1MF}$
PP	storage variable
PPEXIT	p_6'
PPOP1	$(p'/p)_{1MF}$
PR	p_6'/p_0'
PREC1	array of C_p^{**} at area ratio 1.2
PREC2	array of C_p^{**} at area ratio 2.0
PREC3	array of C_p^{**} at area ratio 3.0
PREC4	array of C_p^{**} at area ratio 4.0
PREC5	array of C_p^{**} at area ratio 5.0
PTH	p_5
PTHP	p_5'
Q	Q
QAERO	q_{aero}
R	r
R0P	ρ_0'
R1	ρ_1

22

R1P	ρ_1'
R2	r_3
R2G	$\rho_{3,est}$
RANGE	w_{surge}/w_{choke}
RARRAY	temporary storage
RE	Re
RGAS	R
RHO2	ρ_3
RHOH	ρ_{1H}
RHOMF	ρ_{1MF}
RHOR	ρ/ρ'
RHOT	ρ_{1T}
RMRMS	W_{1MF}/a_1
RTHP	ρ_5'
RVOEST	$\left(\rho V/\rho' V_{cr}\right)_2$
RVORP1	$\left(\rho V/\rho' V_{cr}\right)_1$
RVORVC	$\left(\rho V/\rho' V_{cr}\right)_1 p_1'/p_{iMF}$
RVRVC4	$\left(\rho V/\rho' V_{cr}\right)_6$
RVRVTH	$\left(\rho V/\rho' V_{cr}\right)_5$
S	integral of M^3
SINA	$\sin \alpha_{1T}$
SPLT	splitter control variable
SW	w
T0	T_0
T0P	T_0'
T0PP	T_0''
T1	T_1
T1PP	T_1''

T2	T_3
T2P	T_3'
T2PEST	T_{3est}'
T2PP	T_3''
TALPH	$\tan \alpha$
THETA	θ
TOT0	T_1/T_0
TOT1	T_2/T_1
TPL	p'/p_3'
TX	$\eta_R \, \Delta h_{aero}/C_p T_o' + 1$
U1H	u_{1H}
U1MF	u_{1MF}
U1T	u_{1T}
U2	u_3
V1MF	V_{1MF}
V1T	V_{1T}
V2	V_3
VARAL	$\Delta \tan \alpha$
VARAL1	temporary storage
VARM	ΔM^2
VARM1	temporary storage
VCR	$\left(V_{cr}\right)_0$
VCRTH	$\left(V_{cr}\right)_5$
VLDRR	D_4/D_3
VM1	V_{m1T}
VM1H	V_{m1H}
VM1MF	V_{m1MF}
VM2	V_{m3}
VM1MF	V_{m1MF}

VOVCR	$(V/V_{cr})_0$
VOVCR4	$(V/V_{cr})_6$
VOVCR1	$(V/V_{cr})_1$
VSL	V_{SL}
VU1H	V_{u1H}
Vu1MF	V_{u1MF}
VU1T	V_{u1T}
VU2	V_{u3}
W1H	W_{1H}
W1MF	W_{1MF}
W1MFEF	W_{1MFeff}
W1T	W_{1T}
W2	W_3
W2OW1T	W_3/W_{1T}
WCHK	w_{choke}
WCR	W_{cr}
WFUNC	$w\sqrt{T_3'}/p_5' A_5 B$
W1MF	W_{1MF}
WL	W_L
WOU2	$(w/u_3)^2_{av}$
WSURGE	w_{surge}
WU1H	W_{u1H}
WU1MF	W_{u1MF}
WU1T	W_{u1T}
WU2	W_{u3}
X1	$\alpha - \alpha_4$

XC	K_{vu}
XK	K_{vm}
XM	M
XM1	temporary storage
XM2	M_3
XMACH	M_5
XMARR	array of vaneless diffuser Mach numbers
Z	Z_3
ZETA	ζ

Program Listing

```
DIMENSICN VOVCR(15)
DIMENSICN P3P(20),XMARR(20)
DIMENSION F(20),S(20)
DIMENSICN AMT(4),BARR(6),PREC1(4,6),PREC2(4,6),PREC3(4,6)
DIMENSICN PREC4(4,6),PREC5(4,6)
DIMENSION MWRMS(8),CINC60(8),CINC50(8),CINC40(8)
DIMENSION FLRNG(7),DIFLEM(7)
INTEGER SPLT
REAL LAMX,LCD,MUO,NONDES,MWRMS,INC,N
DATA(AMT(I),I=1,4)/.2,.4,.6,.8/
DATA(BARR(I),I=1,6)/.02,.04,.06,.08,.10,.12/
DATA((PREC1(I,J),I=1,4),J=1,6)/.234,.244,.257,.269,.215,.224,.233,
1.243,.207,.215,.223,.232,.193,.199,.206,.212,.183,.190,.196,.202,.
2169,.176,.182,.188/
DATA((PREC2(I,J),I=1,4),J=1,6)/.644,.670,.696,.722,.620,.638,.656,
1.674,.590,.606,.623,.639,.562,.576,.590,.605,.538,.551,.564,.578,.
2510,.524,.538,.552/
DATA((PREC3(I,J),I=1,4),J=1,6)/.782,.789,.796,.802,.750,.756,.762,
1.768,.708,.716,.724,.732,.672,.680,.687,.695,.652,.648,.654,.660,.
2604,.612,.619,.626/
DATA((PREC4(I,J),I=1,4),J=1,6)/.842,.838,.833,.828,.8,.8,.8,.8,.75
12,.756,.760,.763,.710,.713,.716,.719,.675,.678,.680,.683,.630,.635
2,.640,.646/
DATA((PREC5(I,J),I=1,4),J=1,6)/.878,.865,.852,.838,.832,.825,.818,
1.812,.78,.78,.78,.78,.736,.735,.735,.734,.692,.694,.695,.696,.644,
2.647,.650,.652/
DATA(CINC60(I),I=1,8)/-10.5,-5.,-2.,1.5,2.5,4.,5.,5./
DATA(CINC50(I),I=1,8)/-15.,-7.5,-3.,1.5,4.,6.5,9.,11./
DATA(CINC40(I),I=1,8)/-20.,-12.,-5.,1.5,5.,8.,11.5,14.5/
DATA(MWRMS(I),I=1,8)/.5,.6,.7,.8,.9,1.,1.1,1.2/
DATA(DIFLEM(I),I=1,7)/.4,.5,.6,.7,.8,.9,1./
DATA(FLRNG(I),I=1,7)/.48,.56,.64,.72,.79,.84,.89/
NAMELIST /INPUT/ GAM,POP,TOP,N,DLT,MUO,CF,VOVCR,NVOVCR,RGAS,
1DRAT,LAMX,B2X,Z,VLDRR,B2,B1MFB,AR,BLOCK,AL3,ADTH,NONDES,SPLT,
2 ALIMF,CHIH,CHIT,CURVH,CURVT
1 READ(5,INPUT)
```

```
      WRITE(6,309)
      WRITE(6,315) POF,TOP,MUO,GAM,RGAS
      WRITE(6,310)
      WRITF(6,316) Z,CF,SPLT,N,AL1MF,BLOCK
      WRITE(6,311)
      WRITE(6,317) B1MFB,LAMX,DRAT
      WRITE(6,312)
      WRITE(6,318) B2X,B2,VLDRR,AL3
      WRITE(6,313)
      WRITE(6,319) ADTH,AR
      WRITE(6,314)
      WRITE(6,320) (VOVCR(I),I=1,NVOVCR)
      PERDS=NONDES*100.
      G1=GAM+1.
      G2=GAM-1.
      CP =GAM*RGAS/G2
      B2X=.01745*B2X
      AL3=AL3*.01745
      AL1MF=.01745*AL1MF
      CHIH=.01745*CHIH
      CHIT=.01745*CHIT
      FLFUNC=SQRT(GAM/RGAS*(2./G1)**(G1/G2))
       ROP=POP/RGAS/TOP
      VCR=SQRT(2.*GAM/G1*RGAS*TOP)
      U1T=3.14159*N*NONDES*D1T/60.
      NWRITE=1
      DO 18 L=1,2
      MIN=1
    2 DO 17 J=MIN,NVOVCR
      K=C
      B1MFB=.01745*B1MFB
      VU1T=0.
      VU1MF=0.
      VU1H=0.
      VM1H=VOVCR(J)*VCR
      U2=U1T/DRAT
      D2=D1T/DRAT
      U1H=U1T*LAMX
      D1H=D1T*LAMX
      DMF=SQRT(D1T**2*(1.+LAMX**2)/2.)
      U1MF=U1T*CMF/D1T
      CHIMF=(CHIT-CHIH)*(DMF-D1H)/(D1T-D1H)+CHIH
      CURVMF=(CURVT-CURVH)*(DMF-D1H)/(D1T-D1H)+CURVH
      HO=(CMF-D1H)/2.
      H1=(D1T-DMF)/2.
      FINT=HO/2.*(CURVH+CURVMF)
      AMULT=EXP(FINT)
      VM1MF=AMULT*VM1H
      GINT=(HO+H1)    /6.*((2.-H1/HO)*CURVH+(HO+H1)**2/HO/H1*CURVMF+(2.-HO
     1/H1)*CURVT)
      BMULT=EXP(GINT)
      VM1T=BMULT*VM1H
      VM1HN=VM1H*COS(CHIH)
      VM1MFN=VM1MF*COS(CHIMF)
      VM1TN=VM1T*COS(CHIT)
      RHOH=KOP*(1.-VM1H**2/2./CP/TOP)**(1./G2)
      RHCMF=ROP*(1.-VM1MF**2/2./CP/TOP)**(1./G2)
      RHOT=ROP*(1.-VM1T**2/2./CP/TOP)**(1./G2)
      FCN1=RHOH*VM1HN*D1H/2.
      FCN2=RHCMF*VM1MFN*DMF/2.
```

27

```
      FCN3=RHOT*VM1TN*D1T/2.
      SW=(HO+H1)   /6.*((2.-H1/HO)*FCN1+(HO+H1)**2/HO/H1*FCN2+(2.-HO/H1)*
     1FCN3)*6.28318
      DFIGV=0.
      V1MF=SQRT(VM1MF**2+VU1MF**2)
      T1=TOP-V1MF**2/2./CP
      P1P=POP
      POPP1=(1.-V1MF**2/2./CP/TOP)**(GAM/G2)
      P1=P1P*POPP1
      R1F=P1P/RGAS/TOP
      R1 = R1P*(P1/P1P)**(1./GAM)
      RE=U2*D2/MUO*ROP
      ALSTAG=AL1MF/2.
      FS=0.0076/(COS(AL1MF)-.025)*(1.+COS(ALSTAG)/0.7)
      VOVCR1=VOVCR(J)
      IF(AL1MF.LT.0.001) GO TO 36
    9 VOVCR1=VOVCR1+.001
      AKE=(VOVCR1*VCR)**2/2.
      POPP1=(1.-AKE/CP/TOP)**(GAM/G2)
      AKEID=AKE/(1.-ES)
      P10PPO=(1.-AKEID/CP/TOP)**(GAM/G2)
      P1P=POP*P10PPO/POPP1
      R1F=P1P/RGAS/TOP
      P1=P1P*POPP1
      R1=R1P*(POPP1)**(1./GAM)
      Q1=3.14159*D1T**2*(1.-LAMX**2)*VOVCR1*VCR*COS(AL1MF)/4.
      WTCHK=Q1*R1
      IF(WTCHK.LT.SW) GO TO 9
      VU1MF=VOVCR1*VCR*SIN(AL1MF)
      VM1MF=VOVCR1*VCR*COS(AL1MF)
      V1MF=SQRT(VU1MF**2+VM1MF**2)
      T1=TOP-V1MF**2/2./CP
      XK=VU1MF**2+2.*VM1MF**2
      XC=VU1MF/DMF*2.
      VU1T=XC*D1T/2.
      VU1H=XC*D1H/2.
      VM1T=SQRT(XK-2.*VU1T**2)
      VM1H=SQRT(XK-2.*VU1H**2)
      DFIGV=ES*AKEID
   36 V1T=SQRT(VM1T**2+VU1T**2)
      AL1=ARSIN(VU1T/V1T)
      WU1T=U1T-VU1T
      B1=ATAN(WU1T/VM1T)
      W1T=SQRT(VM1T**2+WU1T**2)
      WU1H=U1H-VU1H
      B1H=ATAN(WU1H/VM1H)
      W1H=SQRT(VM1H**2+WU1H**2)
      A1=SQRT(GAM*RGAS*T1)
      WU1MF=U1MF-VU1MF
      W1MF=SQRT(VM1MF**2+WU1MF**2)
      RMRMS=W1MF/A1
      B1MF=ATAN(WU1MF/VM1MF)
      INC=(B1MF-B1MFB)*57.29577
      EPS=ATAN((1.-BLOCK)*TAN(B1MF)/(1.+BLOCK*(TAN(B1MF))**2))
      BOPT=B1MF-EPS
      T1PP=T1+W1MF**2/2./CP
      WCR=SQRT(2.*GAM/G1*RGAS*T1PP)
      TCTO=1.-G2/G1*(W1MF/WCR)**2
      W1MFEF=W1MF*COS(BOPT-B1MFB)
```

28

```
      TOT1=1.-G2/G1*(W1MFEF/WCR)**2
      TI=T1PP*TOT1
      WL=W1MF*SIN(ABS(BOPT-B1MF))
      DHINC=WL**2/2.
      PIPMF=P1P*EXP(-DHINC/TI/RGAS)
      DELTA=POP/101325.35
      THETA=TOP/288.15
      EWF=SW*SQRT(THETA)/DELTA
      B1MFB=B1MFB*57.29577
      IF(B1MFB.GE.40..AND.B1MFB.LE.50.) GO TO 71
      I=2
81    IF(RMRMS.GE.MWRMS(I-1).AND.RMRMS.LE.MWRMS(I)) GO TO 80
      I=I+1
      GO TO 81
80    CINC1=(RMRMS-MWRMS(I-1))/(MWRMS(I)-MWRMS(I-1))*(CINC60(I)-CINC60(I
     1-1))+CINC60(I-1)
      CINC2=(RMRMS-MWRMS(I-1))/(MWRMS(I)-MWRMS(I-1))*(CINC50(I)-CINC50(I
     1-1))+CINC50(I-1)
      CINC=CINC1+(60.-B1MFB)/10.*(CINC2-CINC1)
      IF(INC.LE.CINC) K=1
      GO TO 74
71    I=2
72    IF(RMRMS.GE.MWRMS(I-1).AND.RMRMS.LE.MWRMS(I)) GO TO 73
      I=I+1
      GO TO 72
73    CINC1=(RMRMS-MWRMS(I-1))/(MWRMS(I)-MWRMS(I-1))*(CINC50(I)-CINC50(I
     1-1))+CINC50(I-1)
      CINC2=(RMRMS-MWRMS(I-1))/(MWRMS(I)-MWRMS(I-1))*(CINC40(I)-CINC40(I
     1-1))+CINC40(I-1)
      CINC=CINC1+(50.-B1MFB)/10.*(CINC2-CINC1)
      IF(INC.LE.CINC) K=1
74    CONTINUE
      IF(K.EQ.1.AND.J.EQ.1) GO TO 202
      IF(K.EQ.1.AND.L.EQ.1) GO TO 18
      T2PP=T1PP+(U2**2-U1MF**2)/2./CP
      PHI=VM1MF/U2
      EPSLIM=1./EXP(8.16*COS(B2X)/Z)
      VSL=SQRT(COS(B2X))*U2/Z**.7
      IF((DMF/D2).GT.EPSLIM) VSL=U2*(SQRT(COS(B2X))/Z**.7)*(1.-((DMF/D2-
     1EPSLIM)/(1.-EPSLIM))**3)+U2*((DMF/D2-EPSLIM)/(1.-EPSLIM))**3
      DHEST=U2**2
      T2PEST=(DHEST/CP/TOP+1.)*TOP
      R2G=R1*(T2PEST/TOP)**(1./G2)
4     RHO2=R2G
      VM2=SW/(3.14159*RHO2*D2*B2)
      VU2=U2-VM2*TAN(B2X)-VSL
      MIN=J
      IF(VM2.LT.0..AND.L.EQ.2) GO TO 200
      IF(VM2.LT.0.) GO TO 17
      IF(VU2.LT.0..AND.L.EQ.2) GO TO 201
      IF(VU2.LT.0.) GO TO 17
      WU2=U2-VU2
      W2=SQRT(WU2**2+VM2**2)
      IF((VSL*COS(B2X)/W2).GT.1..AND.L.EQ.2) GO TO 202
      IF((VSL*COS(B2X)/W2).GT.1.) GO TO 17
      T2=T2PP-W2**2/2./CP
      A2=SQRT(GAM*RGAS*T2)
      W2OW1T=W2/W1T
      WOU2=(PHI**2+(DMF/D2)**2+W2OW1T**2*(PHI**2+DRAT**2))/2.
```

```
      AL2=ATAN(VU2/VM2)
      V2=SQRT(VU2**2+VM2**2)
      T2P=T2+V2**2/2./CP
      DHAERO=CP*TOP*(T2P/TOP-1.)
      QAERO=DHAERO/U2**2
      DF=   W1T/U2*(Z/3.14159*(1.-D1T/D2)+2.*D1T/D2)
      CONST1=0.75
      IF(SPLT.EC.1) CONST1=0.6
      DF=1.-W2DW1T+CONST1*QAERO/CF
      DHBL=0.05*DF**2*U2**2
      LOD=(1.-DMF/.3048)/COS(B2X)/2.
      DHDF=.01356*RHO2*U2**3*D2**2/SW/RE**.2
      DHYD=Z/3.14159/COS(B2X)+D2/B2
      DFYD=1./DHYD+D1T/D2/(2./(1.-LAMX)+2.*Z/3.14159/(1.+LAMX)
     1*SQRT(1.+(1.+LAMX**2)/2.*(TAN(B1))**2))
      DHRC=0.02*SQRT(TAN(AL2))*DF**2*U2**2
      CONST2=5.6
      IF(SPLT.EC.1) CONST2=7.0
      DHSF=CONST2*CF*LOD/DHYD*W0U2*U2**2
      DHACT=CHAERO+DHDF+DHRC
      HIS=DHAERO-DHBL-DHSF-DHIGV-DHINC
      ETAR=HIS/DHAERO
      TX=ETAR*DHAERO/CP/TOP+1.
   51 P2P=TX**(GAM/G2)*PIPMF
      P2=P2P*(T2P/T2)**(-GAM/G2)
      R2G=P2/RGAS/T2
      IF(ABS((RHO2-R2G)/RHO2).GT.0.001) GO TO 4
      XM2= V2/A2
      R2=D2/2.
      AMU=1.4579E-6*T2**1.5/(T2+110.4)
      ANU=AMU/R2G
      BO=1.
      XM=XM2
      ALPHA=AL2
      R=1.0
      F(1)=XM2**3/(1.+G2/2.*XM2**2)**(G1/2./G2)
      P3P(1)=P2P
      XMARR(1)=XM2
      DELTAR=(VLDRR-1.)/10.
      ZETA=CF*R2/B2
      AS=0.
      DC 1000 NO=2,10
      XM1=XM
      ALPH1=ALPHA
      DS=DELTAR*R2/COS(ALPHA)
      AS=AS+DS
      DELTAS=.037*AS**(-.2)*(V2/ANU)**(-.2)*DS
      B=BO-2.*DELTAS/B2
      DELTAB=BO-B
      VARM=-2.*(1.+G2/2.*XM**2)/(XM**2-1./COS(ALPHA)**2)*((GAM*XM**2-TAN
     1(ALPHA)**2)*ZETA/BO/COS(ALPHA)+1./BO*DELTAB/DELTAR-1./COS(ALPHA)**
     22/R)*XM**2*DELTAR
      VARAL=1./COS(ALPHA)**2/(XM**2-(1./COS(ALPHA))**2)*((1.+G2   *XM**2
     1)*ZETA/BO/COS(ALPHA)+1./BO*DELTAB/DELTAR-XM**2/R)*TAN(ALPHA)*DELTA
     2R
      VARM1=VARM
      VARAL1=VARAL
      B1=B
      B=BO
```

```
      AS=AS-DS
      XM=XM1**2+VARM
      XM=SORT(XM)
      TALPH=TAN(ALPH1)+VARAL1
      ALPHA=ATAN(TALPH)
      DS=DELTAR*R2/COS(ALPHA)
      R=R+DELTAR
      AS=AS+DS
      DELTAS=.037*AS**(-.2)*(V2/ANU)**(-.2)*DS
      B=B0-2.*DELTAS/B2
      DELTAB=B0-B
      VARM=-2.*(1.+G2/2.*XM**2)/(XM**2-1./COS(ALPHA)**2)*((GAM*XM**2-TAN    A
     1(ALPHA)**2)*ZETA/B0/COS(ALPHA)+1./B0*DELTAB/DELTAR-1./COS(ALPHA)**
     22/R)*XM**2*DELTAR
      VARAL=1./COS(ALPHA)**2/(XM**2-(1./COS(ALPHA))**2)*((1.+G2    *XM**2
     1)*ZETA/B0/COS(ALPHA)+1./B0*DELTAB/DELTAR-XM**2/R)*TAN(ALPHA)*DELTA
     2R
      VARM=(VARM1+VARM)/2.
    7 VARAL=(VARAL1+VARAL)/2.
      B=(B+R1)/2.
      XM=XM1**2+VARM
      XM=SORT(XM)
      TALPH=TAN(ALPH1)+VARAL
      ALPHA=ATAN(TALPH)
      B0=B
      ACCUSR=SORT(1./(1.+G2/2.*XM**2))
      RHOR=1./(1.+G2/2.*XM**2)**(1./G2)
      F(NO)=XM**3*ACCUSR*RHOR*R
      IF(NO.EQ.2) S(NO)=(F(NO)+F(NO-1))*0.5*DELTAR
      IF(NO.EQ.2) GO TO 8
      CALL FNTGRL(NO,DELTAR,F,S)
    8 TPL=1./(1.+GAM*CF*R2*S(NO)/COS(AL2)/B2/XM2*(1.+G2/2.*XM2**2)**(G1/
     12./G2))
      PP=TPL*P2P
      P3P(NO)=PP
      XMARR(NO)=XM
      XMACH=XMARR(NO)
 1000 PTHP=P3P(NO)
      IF(L.EQ.1) GO TO 30
      M=2
   21 IF(XMACH.GE.DIFLEM(M-1).AND.XMACH.LE.DIFLEM(M)) GO TO 22
      M=M+1
      GO TO 21
   22 RANGE=(XMACH-DIFLEM(M-1))/(DIFLEM(M)-DIFLEM(M-1))*(FLRNG(M)-FLRNG(
     1M-1))+FLRNG(M-1)
      WSURGE=RANGE*WCFK
      IF(EWF.LT.WSURGE) GO TO 203
   30 CONTINUE
      PTH=PTHP/(1.+G2/2.*XMACH**2)**(GAM/G2)
      DHVLD=CP*T2P*((PTH/PTHP)**(G2/GAM)-(PTH/P2P)**(G2/GAM))
      BT=1.-B
      XMACH=XMACH*COS(ABS(ALPHA-AL3))
      PTHP=PTH*(1.+G2/2.*XMACH**2)**(GAM/G2)
      X1=(ALPHA-AL3)*57.29577
      WFUNC=SW*SORT(T2P)/ADTH/PTHP/B
      IF(WFUNC.GE.FLFUNC) CPSTAR=0.
      IF(WFUNC.GE.FLFUNC) K=1
      IF(WFUNC.GE.FLFUNC) GO TO 14
      IF ((AR-1.2).GT.0..AND.(AR-2.).LT.0.) GO TO 10
      IF ((AR-2.).GT.0..AND.(AR-3.).LT.0.) GO TO 11
```

```
      IF ((AR-3.).GT.0..AND.(AR-4.).LT.0.) GO TO 12
      IF ((AR-4.).GT.0..AND.(AR-5.).LT.0.) GO TO 13
   10 CALL LININT(XMACH,BT,AMT,BARR,PREC1,4,6,F1)
      CALL LININT(XMACH,BT,AMT,BARR,PREC2,4,6,F2)
      CPSTAR=(AR-1.2)/.8*(F2-F1)+F1
      GC TO 14
   11 CALL LININT(XMACH,BT,AMT,BARR,PREC2,4,6,F2)
      CALL LININT(XMACH,BT,AMT,BARR,PREC3,4,6,F3)
      CPSTAR=(AR-2.)*(F3-F2)+F2
      GO TO 14
   12 CALL LININT(XMACH,BT,AMT,BARR,PREC3,4,6,F3)
      CALL LININT(XMACH,BT,AMT,BARR,PREC4,4,6,F4)
      CPSTAR=(AR-3.)*(F4-F3)+F3
      GO TO 14
   13 CALL LININT(XMACH,BT,AMT,BARR,PREC4,4,6,F4)
      CALL LININT(XMACH,BT,AMT,BARR,PREC5,4,6,F5)
      CPSTAR=(AR-4.)*(F5-F4)+F4
   14 CCNTINUE
      IF(K.EO.1.AND.J.EO.1) GO TO 202
      IF(K.EO.1.AND.L.EO.1) GO TO 18
      IF(K.NE.1.AND.J.EO.NVOVCR) GO TO 204
      PEXIT=CPSTAR*(PTHP-PTH)+PTH
      RTHP=PTHP/RGAS/T2P
      VCRTH=SQRT(2.*GAM/G1*RGAS*T2P)
      RVRVTH=SW/RTHP/VCRTH/ADTH/B
      VOVCR4=.020
  100 P4PL=PEXIT/(1.-G2/G1*VOVCR4**2)**(GAM/G2)
      RVRVC4=(1.-G2/G1*VOVCR4**2)**(1./G2)*VOVCR4
      P4PG=RVRVTH*PTHP/AR/RVRVC4
      VCVCR4=VOVCR4+.001
      IF(P4PL.LT.P4PG) GO TO 100
      PPEXIT=P4PG
   15 DHCIF=T2P*CP*((PEXIT/PPEXIT)**(G2/GAM)-(PEXIT/PTHP)**(G2/GAM))
      PR=PPEXIT/POP
      ETAD=DHAERO-DHSF-CHBL-DHVLD-DHDIF-DHIGV-DHINC
      ETAD=ETAD/DHACT
      DEIGV=DHIGV/DHACT
      DEBL=DHBL/DHACT
      DESF=DHSF/DHACT
      DEDF=DHDF/DHACT
      DERC=DHRC/DHACT
      DEVLD=DHVLD/DHACT
      DEVD=DHDIF/DHACT
      DEINC=DHINC/DHACT
      IF(L.EO.2) GO TO 19
   17 CCNTINUE
      IF(L.EO.1) GO TO 18
   19 IF(NWRITE.NE.1) GO TO 35
      WRITE(6,300)
      WRITE(6,301) PERDS
      WRITE(6,302)
      WRITE(6,303) WSURGE,WCHK
      NWRITE=NWRITE+1
   35 MIN=MIN+1
      WRITE(6,304)
      WRITE(6,305) EWF,PR,ETAD
      WRITE(6,306)
      WRITE(6,307) DEIGV,DEINC,DEBL,DESF,DEDF,DERC,DEVLD,DEVD
      IF(K.NE.1.AND.MIN.LE.NVOVCR) GO TO 2
```

32

```
      IF(K.EQ.1.AND.L.EQ.2) GO TO 1
200 WRITE(6,400)
      MIN=MIN+1
      IF(MIN.GT.NVOVCR) GO TO 1
      GO TO 2
201 WRITE(6,400)
      MIN=MIN+1
      IF(MIN.GT.NVOVCR) GO TO 1
      GO TO 2
202 WRITE(6,402)
      GO TO 1
203 WRITE(6,403) VOVCR(J)
      MIN=MIN+1
      IF(MIN.GT.NVOVCR) GO TO 1
      GO TO 2
204 WRITE(6,308)
      GO TO 1
  18 WCHK=SW*SQRT(THETA)/DELTA
      GO TO 1
300 FORMAT(59X,13H PERCENT NDES)
301 FORMAT(63X,F5.1)
302 FORMAT(45X,16H SURGE FLOW RATE,10X,15HCHOKE FLOW RATE)
303 FORMAT(51X,F5.3,20X,F5.3)
304 FORMAT(44X,4H WEQ,10X,14HPRESSURE RATIO,10X,4HETAT)
305 FORMAT(44X,F5.3,13X,F5.3,15X,F4.3)
306 FORMAT(11X,8H DETAIGV,8X,7HDETAINC,8X,6HDETABL,8X,6HDETASF,8X,6HDE
     1TADF,8X,6HDETARC,8X,7HDETAVLD,8X,6HDETAVD)
307 FORMAT(13X,F6.5,9X,F6.5,8X,F6.5,8X,F6.5,8X,F6.5,8X,F6.5,9X,F6.5,
     18X,F6.5,9X,F6.5)
308 FORMAT(45H COMPRESSOR CHOKING FLOW HAS NOT BEEN REACHED)
309 FORMAT(21H1INLET TOTAL PRESSURE,5X,23HINLET TOTAL TEMPERATURE,5X,2
     19HINLET TOTAL DYNAMIC VISCOSITY,5X,19HSPECIFIC HEAT RATIO,5X,12HGA
     2S CONSTANT)
310 FORMAT(17H NUMBER OF BLADES,5X,20HFRICTION CCEFFICIENT,5X,4HSPLT,5
     1X,12HDESIGN SPEED,5X,23HINDUCER RMS SWIRL ANGLE,5X,27HINDUCER RMS
     2BLOCKAGE FACTOR)
311 FORMAT(11X,24H INDUCER RMS BLADE ANGLE,5X,30HINDUCER HUB-TIP DIAME
     1TER RATIO,5X,40HINDUCER TIP-IMPELLER EXIT DIAMETER RATIO)
312 FORMAT(30H IMPELLER BLADE EXIT BACKSWEEP,5X,23HIMPELLER BLADE EXIT
     1 HT.,5X,32HVANELESS DIFFUSER DIAMETER RATIO,5X,28HVANED DIFFUSER S
     2ETTING ANGLE)
313 FORMAT(33X,33H TOTAL VANED DIFFUSER THROAT AREA,5X,25HVANED DIFFUS
     1ER AREA RATIO)
314 FORMAT(47X,36H INLET CRITICAL VELOCITY RATIO ARRAY)
315 FORMAT(7X,F7.0,21X,F6.2,23X,F8.7,24X,F3.1,16X,F6.2)
316 FORMAT(7X,F3.0,20X,F4.3,15X,I1,9X,F6.0,17X,F4.2,26X,F4.2)
317 FORMAT(24X,F4.1,27X,F6.4,34X,F6.4)
318 FORMAT(13X,F4.1,26X,F6.5,27X,F6.3,30X,F5.2)
319 FORMAT(47X,F7.6,28X,F4.2)
320 FORMAT(8F10.2)
400 FORMAT(1X,24HIRRATIONAL EXIT TRIANGLE)
402 FORMAT(1X,21HVOVCR ARRAY TOO LARGE)
403 FORMAT(1X,34HWT FLOW LESS THAN SURGE FOR V/VCR=,F4.2)
      END
```

Subroutine LININT(X1, Y1, X, Y, TN, MX, MY, F)

This subroutine interpolates a value of maximum pressure recovery coefficient C_p^{**} from a table of vaned diffuser throat Mach numbers and aerodynamic blockage given as input.

X1   input, vaned diffuser throat Mach number

Y1   input, throat aerodynamic blockage

X   input array of throat Mach numbers

Y   input array of throat blockages

TN   input two-dimensional array of C_p^{**} corresponding to throat Mach numbers and blockages

MX   input, number of throat Mach numbers

MY   input, number of throat blockages

F   output, interpolated value of C_p^{**}

```
$IBFTC LININT
      SUBROUTINE LININT (X1,Y1,X,Y,TN,MX,MY,F)
      DIMENSION X(MX), Y(MY), TN(MX,MY)
      DO 1 J3=2,MX
1     IF (X1.LE.X(J3)) GO TO 2
      J3=MX
2     DO 3 J4=2,MY
3     IF (Y1.LE.Y(J4)) GO TO 4
      J4=MY
4     J1=J3-1
      J2=J4-1
      EPS1=(X1-X(J1))/(X(J3)-X(J1))
      EPS2=(Y1-Y(J2))/(Y(J4)-Y(J2))
      EPS3=1.-EPS1
      EPS4=1.-EPS2
      F=TN(J1,J2)*EPS3*EPS4+TN(J3,J2)*EPS1*EPS4+TN(J1,J4)*EPS2*EPS3+TN(J
     13,J4)*EPS1*EPS2
      RETURN
      END
```

Subroutine FNTGRL(NO, DELTAR, F, S)

This subprogram is used to integrate the function $M^3(\rho a/\rho' a')$ in the vaneless diffuser.

34

NO   number of equally spaced radii

DELTAR   radius ratio between stations

F   function $M^3(\rho a/\rho'a')$

S   integral of F

No FORTRAN listing of the subprogram is available but a brief description of the method of integration is as follows:

The subprogram uses Simpson's rule in the following manner:

First interval:

$$\int_{x_1}^{x_1} f(x)dx = 0$$

Second interval:

$$\int_{x_1}^{x_2} f(x)dx = \Delta x(5f_1 + 8f_2 - f_3)/12$$

Remaining intervals:

$$\int_{x_i}^{x_{i+1}} f(x)dx = \Delta x(5f_{i+1} + 8f_i - f_{i-1})/12$$

Lewis Research Center,
    National Aeronautics and Space Administration,
        and
U.S. Army Air Mobility R&D Laboratory,
    Cleveland, Ohio, August 2, 1973,
        501-24.

SYMBOLS

A	area, m^2
AR	area ratio
a	local acoustic velocity, m/sec
B	effective depth ratio
b	blade height or passage depth, m
C	wall curvature, m^{-1}
C_f	skin friction coefficient
C_p	specific heat, J/(kg)(K)
C_p^{**}	maximum pressure recovery coefficient at a constant area ratio
D	diameter, m
D_f	diffusion factor
e_s	inlet guide vane loss coefficient
h	spacing for numerical integration
Δh	incremental compressor specific enthalpy, J/kg
K	constant
L	blade length, m
M	Mach number
N	rotative speed, rpm
n	distance along radius, m
p	pressure, N/m^2
Q	volumetric flow rate, m^3/sec
q	dimensionless enthalpy
R	gas constant, J/(kg)(K)
$\bar{R}$	radius ratio
Re	Reynolds number based on inlet total conditions
r	radius, m
s	arc length, m

Δs	incremental arc length, m
T	temperature, K
t	blade thickness, m
u	blade speed, m/sec
V	absolute gas velocity, m/sec
W	relative gas velocity, m/sec
w	mass flow rate, kg/sec
Z	number of impeller blades
α	absolute flow angle, deg from meridional plane
β	relative flow angle, deg from meridional plane
β_b	blade angle, deg from meridional plane
γ	specific heat ratio
δ	ratio of inlet total pressure to standard sea-level pressure
$\Delta\delta^*$	incremental boundary layer displacement thickness, m
ϵ	difference between compressor inlet relative flow angle and optimum incidence angle
ζ	vaneless diffuser loss coefficient
η	total efficiency
$\Delta\eta$	total efficiency decrement
θ	ratio of inlet total temperature to standard sea-level temperature
λ	inducer hub-tip diameter ratio
μ	dynamic viscosity, N-sec/m^2
ν	kinematic viscosity, $\text{m}^2\text{/sec}$
ρ	gas density, kg/m^3
φ	flow coefficient
χ	wall slope or streamline angle, deg from axial

Subscripts:

act	actual
AD	adiabatic
aero	aerodynamic

av	average
BL	blade loading
calc	calculated
choke	value at choking flow rate
cr	critical condition
DES	design
DF	disk friction
eff	effective
eq	equivalent
est	estimated
exit	exit
H	hub
HYD	hydraulic
i	iteration subscript
id	ideal
IGV	inlet guide vane
INC	incidence
is	isentropic
L	lost
m	meridional
max	maximum
MF	rms
n	normal
opt	optimum
R	rotor
RC	recirculation
SF	skin friction
SL	slip
st	stagger
surge	value at surge flow rate

38

T	tip
u	tangential
v	vortex
VD	vaned diffuser
VLD	vaneless diffuser
0	station just upstream of inlet guide vanes
1	impeller inlet upstream of blade
2	impeller inlet just downstream of blade leading edge
3	impeller exit
4	vaned diffuser leading edge
5	vaned diffuser throat
6	vaned diffuser exit

Superscripts:

'	absolute total condition
''	relative total condition

APPENDIX B

EQUATIONS

This section presents a more detailed discussion of the method of calculating compressor performance than was presented in the section Method of Analysis.

The equations used in calculating the flow solution through the compressor are listed here in the approximate order of solution in the FORTRAN program. The known constants are the input fluid state and thermodynamic properties, compressor geometry, and velocity diagram data. The working fluid properties and state conditions are specific heat ratio γ, inlet total pressure p_0', inlet total temperature T_0', and inlet dynamic viscosity based on total conditions μ_0'. The velocity diagram data are compressor design rotative speed N_{DES}, the fraction of design rotative speed for which performance data is desired N/N_{DES}, the number of values of $\left(V/V_{cr}\right)_0$ for which performance is to be calculated, the values of $\left(V/V_{cr}\right)_0$ to be used, and the inducer solid-body swirl angle at the rms diameter α_{1MF}. The compressor data are inducer inlet hub and tip wall slopes χ_{1H} and χ_{1T}, inducer inlet hub and tip wall curvatures C_{1H} and C_{1T}, inducer inlet tip diameter D_{1T}, inducer inlet hub-tip diameter ratio λ, inducer-inlet-tip to impeller-exit diameter ratio D_{1T}/D_3, number of blades at impeller exit (including splitters) Z_3, impeller blade exit angle (positive opposite to direction of rotation) β_{3b}, impeller exit blade height b_3, inducer inlet blade angle at the rms diameter β_{1MFb}, inducer inlet blockage factor calculated at the rms diameter, vaneless diffuser diameter ratio D_4/D_3, vaned diffuser setting angle α_4, total vaned diffuser throat area A_5, vaned diffuser area ratio A_6/A_5, and wetted surface friction coefficient C_f. With these known values compressor performance can be evaluated by the method described.

Calculation of Inlet Velocity Triangles and Compressor Weight Flow

Calculation of the inducer inlet velocity diagrams and weight flow are handled by two methods depending on whether the inlet is swirl-free or subject to solid-body swirl. For the swirl cases it is assumed that the inlet guide vanes are located in a constant area annulus with zero wall slope with respect to the axial direction. The inner and outer diameters of the annulus are assumed to be equal to the inducer inlet hub and tip diameters. For the swirl-free cases it is assumed that the flow orthogonal can be approximated by a radial line. These assumptions greatly simplify calculation of the velocities specified by the general velocity gradient equation.

40

<u>Swirl-free inlets</u>. - For compressor configurations with swirl-free inlets the input value of $\left(V/V_{cr}\right)_0$ is used as the hub streamline value of V/V_{cr}. The variation of inlet velocity with radius is calculated from the general velocity gradient equation simplified for swirl-free flow. This equation is (in simplified form from ref. 10)

$$V_m = V_{m1H}\, e^{\int_0^n C\, dn} \qquad (B1)$$

where V_{m1H} is the hub absolute velocity, C is the streamline curvature, and n is the distance along a radius. Streamline curvature and slope at the rms inlet diameter are approximated by linear interpolation of the input hub and tip values. The integral in the previous equation is approximated by the trapezoidal rule at the rms diameter and by Simpson's rule for unequal intervals at the tip. The numerical approximations are

$$V_{m1MF} = V_{m1H}\, e^{\left[\frac{h_0}{2}(C_{1H}+C_{1MF})\right]} \qquad (B2)$$

and

$$V_{m1T} = V_{m1H}\, e^{\left\{\left(\frac{h_0+h_1}{6}\right)\left[\left(2-\frac{h_1}{h_0}\right)C_{1H}+\frac{(h_0+h_1)^2}{h_1 h_0}C_{1MF}+\left(2-\frac{h_0}{h_1}\right)C_{1T}\right]\right\}} \qquad (B3)$$

where

$$h_0 = r_{1MF} - r_{1H} \qquad (B4)$$

and

$$h_1 = r_{1T} - r_{1MF} \qquad (B5)$$

Static densities at the hub, rms, and tip diameters are determined from the inlet total density and the calculated velocity at each station. Velocity components normal to the annular inlet plane are calculated using the velocities and streamline angles at the three stations:

$$V_{m1n} = V_{m1} \cos \chi \qquad (B6)$$

where χ is the streamline angle. Inlet mass flow is then computed using Simpson's rule for unequal intervals

$$w = 2\pi \left\{ \frac{h_0 + h_1}{6} \left[\left(2 - \frac{h_1}{h_0} \right) (\rho r)_{1H} V_{m1Hn} + \frac{(h_0 + h_1)^2}{h_0 h_1} (\rho r)_{1MF} V_{m1MFn} \right. \right.$$

$$\left. \left. + \left(2 - \frac{h_0}{h_1} \right) (\rho r)_{1T} V_{m1Tn} \right] \right\} \qquad (B7)$$

Inlets with solid-body swirl. - For impeller inlets with inlet guide vanes producing solid-body swirl the equations presented in reference 2 for kinetic energy loss were iteratively solved for state conditions and velocities downstream of the inlet guide vanes. Conditions at the rms diameter were assumed to be representative of the flow distribution at the impeller inlet. The inlet guide vane stagger angle was assumed to be one-half of the turning angle at the rms diameter; that is,

$$\alpha_{ST} = \frac{\alpha_{1MF}}{2} \qquad (B8)$$

The inlet guide vane loss coefficient was calculated from the equation

$$e_S = \frac{0.0076}{\cos \alpha_{1MF} - 0.025} \left(1 + \frac{\cos \alpha_{ST}}{0.7} \right) \qquad (B9)$$

Using the input value of $\left(V/V_{cr} \right)_0$ as a first approximation to the value of V/V_{cr} downstream of the inlet guide vanes at the rms diameter, the following equations are solved iteratively with successive increments in V/V_{cr} until continuity checks the calculation of equation (B7):

42

$$KE = \frac{\left(\dfrac{V}{V_{cr}} V_{cr}\right)^2}{2} \tag{B10}$$

$$\left(\frac{p}{p'}\right)_{1MF} = \left(1 - \frac{KE}{C_1 T'_0}\right)^{\gamma/(\gamma-1)} \tag{B11}$$

$$KE_{id} = \frac{KE}{1 - e_S} \tag{B12}$$

$$\frac{p_{1MF}}{p'_0} = \left(1 - \frac{KE_{id}}{C_p T'_0}\right)^{\gamma/(\gamma-1)} \tag{B13}$$

$$p'_{1MF} = p'_0 \frac{\dfrac{p_{1MF}}{p'_0}}{\left(\dfrac{p}{p'}\right)_{1MF}} \tag{B14}$$

$$\rho'_{1MF} = \frac{p'_{1MF}}{R T'_0} \tag{B15}$$

$$p_{1MF} = p'_{1MF} \left(\frac{p}{p'}\right)_{1MF} \tag{B16}$$

$$\rho_{1MF} = \rho'_{1MF} \left(\frac{p}{p'}\right)_{1MF}^{1/\gamma} \tag{B17}$$

$$Q_1 = \frac{\pi}{4} D_{1T}^2 (1 - \lambda^2) \left(\frac{V}{V_{cr}}\right)_{1MF} V_{cr} \cos \alpha_{1MF} \tag{B18}$$

$$w = Q_1 \rho_{1MF} \tag{B19}$$

43

When continuity is satisfied downstream of the inlet guide vanes, the impeller inlet velocity triangles are calculated. Combination of the Euler equation with the solid-body vortex equation and simple radial equilibrium equation shows that the meridional velocity distribution can be expressed as

$$V_{m1} = \sqrt{K_{Vm} - 2V_{u1}^2} \qquad (B20)$$

Using the value of V/V_{cr} which satisfies continuity downstream of the inlet guide vanes and the input value of the rms turning angle allows solution of the constant in equation (B20). The tangential components of the inlet absolute velocity at the hub and tip are calculated from the vortex condition. Then the hub and tip meridional velocities can be determined as follows:

$$V_u = K_{Vu} r \qquad (B21)$$

where

$$K_{Vu} = \frac{V_{u1MF}}{r_{1MF}} \qquad (B22)$$

The following general inducer inlet velocity diagram characteristics are calculated after the particular swirl-free or solid-body swirl calculations are completed:

$$V_{1T} = \sqrt{V_{m1T}^2 + V_{u1T}^2} \qquad (B23)$$

$$\alpha_{1T} = \sin^{-1}\left(\frac{V_{u1T}}{V_{1T}}\right) \qquad (B24)$$

$$W_{u1T} = u_{1T} - V_{u1T} \qquad (B25)$$

$$\beta_{1T} = \tan^{-1}\left(\frac{W_{u1T}}{V_{m1T}}\right) \qquad (B26)$$

44

$$W_{1T} = \sqrt{V_{m1T}^2 + W_{u1T}^2} \qquad (B27)$$

$$W_{u1H} = u_{1H} - V_{u1H} \qquad (B28)$$

$$\beta_{1H} = \tan^{-1}\left(\frac{W_{u1H}}{V_{m1H}}\right) \qquad (B29)$$

$$W_{1H} = \sqrt{V_{m1H}^2 + W_{u1H}^2} \qquad (B30)$$

$$V_{1MF} = \sqrt{V_{u1MF}^2 + V_{m1MF}^2} \qquad (B31)$$

$$W_{u1MF} = u_{1MF} - V_{u1MF} \qquad (B32)$$

$$W_{1MF} = \sqrt{V_{m1MF}^2 + W_{u1MF}^2} \qquad (B33)$$

$$\beta_{1MF} = \tan^{-1}\left(\frac{W_{u1MF}}{V_{m1MF}}\right) \qquad (B34)$$

The wheel speeds used in the previous equations are obtained from the following input constants:

$$u_{1T} = \frac{\pi\left(\dfrac{N}{N_{DES}}\right)N_{DES}D_{1T}}{60} \qquad (B35)$$

$$u_{1H} = \lambda u_{1T} \qquad (B36)$$

$$u_{1MF} = u_{1T}\,\frac{D_{1MF}}{D_{1T}} \qquad (B37)$$

45

where

$$D_{1MF} = \sqrt{\frac{1}{2} D_{1T}^2 (1 + \lambda^2)} \qquad (B38)$$

Individual Losses

Inlet guide vane loss. - When the inducer inlet velocity diagram characteristics have been determined by the method described in the section Inlets With Solid-Body Swirl, the inlet guide vane loss is computed using the equation found in reference 1, subject to the assumptions made in reference 3.

$$\Delta h_{IGV} = e_s KE_{id} \qquad (B39)$$

Inducer incidence loss. - The equations developed in reference 4 are used to determine the optimum inducer incidence angle for incompressible flow. Compressibility effects are ignored because the incidence loss is evaluated at the rms diameter and compressibility effects are insignificant except at the hub according to reference 4. Using the input blade blockage factor at the rms diameter the optimum incidence angle is found by

$$\epsilon = \tan^{-1} \frac{(1 - B_1)\tan \beta_{1MF}}{1 + B_1 \tan^2 \beta_{1MF}} \qquad (B40)$$

where

$$B_1 = 1 - \frac{Z_1 t_u}{2\pi r_{1MF}} \qquad (B41)$$

The optimum relative flow angle is then

$$\beta_{opt} = \beta_{1MF} - \epsilon \qquad (B42)$$

and the component of the relative velocity lost is

46

$$W_L = W_{1MF} \sin |\beta_{opt} - \beta_{1MF}|$$
(B43)

The enthalpy loss due to incidence is expressed as

$$\Delta h_{INC} = \frac{W_L^2}{2C_p}$$
(B44)

and the total pressure just inside the blade row is

$$p'_{2MF} = p'_{1MF} \, e^{\left(\frac{-\Delta h_{INC}}{T_2 R}\right)}$$
(B45)

Impeller work and losses. - The impeller exit density is obtained through iteration of the impeller loss equations and calculated state properties. The enthalpy rise in the impeller is initially approximated as

$$\Delta h_{est} = u_3^2$$
(B46)

and the corresponding impeller exit total temperature is then

$$T'_{3est} = \left(\frac{\Delta h_{est}}{C_p T'_0} + 1\right) T'_0$$
(B47)

The impeller exit density is initially approximated to be

$$\rho_3 = \rho_{1MF} \left(\frac{T'_{3est}}{T'_0}\right)^{1/(\gamma - 1)}$$
(B48)

The meridional component of exit absolute velocity is calculated from continuity

$$V_{m3} = \frac{w}{\pi \rho_3 D_3 b_3}$$
(B49)

The tangential component of exit absolute velocity is then

$$V_{u3} = u_3 - V_{m3} \tan \beta_{3b} - V_{SL} \tag{B50}$$

where the slip velocity V_{SL} is calculated by the method of reference 11.

$$V_{SL} = \frac{u_3 \sqrt{\cos \beta_{3b}}}{z_3^{0.7}} \tag{B51}$$

The remaining state and flow properties at the exit were calculated from the following relations:

$$T_3'' = T_{1MF}'' + \frac{u_3^2 - u_{1MF}^2}{2C_p} \tag{B52}$$

$$W_{u3} = u_3 - V_{u3} \tag{B53}$$

$$W_3 = \sqrt{V_{m3}^2 + W_{u3}^2} \tag{B54}$$

$$T_3 = T_3'' - \frac{W_3^2}{2C_p} \tag{B55}$$

$$V_3 = \sqrt{V_{m3}^2 + V_{u3}^2} \tag{B56}$$

$$T_3' = T_3 + \frac{V_3^2}{2C_p} \tag{B57}$$

The work loss due to blade loading is calculated from the equation

$$\Delta h_{BL} = 0.05 \, D_f^2 u_3^2 \tag{B58}$$

which is given by reference 5. The diffusion factor D_f is defined as

48

$$D_f = 1 - \frac{W_3}{W_{1T}} + \frac{K_{BL} q_{aero}}{\frac{W_{1T}}{u_3} \left[\frac{Z_3}{\pi} \left(1 - \frac{D_{1T}}{D_3} \right) + 2 \frac{D_{1T}}{D_3} \right]} \qquad \text{(B59)}$$

where a value of 0.75 is used for K_{BL} for conventional impellers and a value of 0.6 is used for impellers with splitters. A parametric study of calculated diffusion factors with a variation in the number of blades indicated that changing the constant to 0.6 would compensate for the changing solidity near the exit. The dimensionless actual head is obtained by dividing the enthalpy rise by the exit blade speed squared

$$q_{aero} = \frac{\Delta h_{aero}}{u_3^2} \qquad \text{(B60)}$$

where

$$\Delta h_{aero} = C_p T_0' \left(\frac{T_3'}{T_0'} - 1 \right) \qquad \text{(B61)}$$

Impeller disk friction loss is computed using the method of reference 6

$$\Delta h_{DF} = 0.01356 \frac{\rho_3}{w Re^{0.2}} u_3^3 D_3^2 \qquad \text{(B62)}$$

The Reynolds number in this equation is based on impeller exit dimensions and inlet total conditions

$$Re = \frac{u_3 D_3 \rho_{1MF}'}{\mu_0'} \qquad \text{(B63)}$$

Skin friction loss is calculated from the correlation found in reference 5

$$\Delta h_{SF} = K_{SF} C_f \frac{\dfrac{L}{D_3}}{\dfrac{D_{HYD}}{D_3}} \left(\frac{W}{u_3}\right)^2_{av} u_3^2 \qquad (B64)$$

where the mean flowpath blade length-diameter ratio is expressed as

$$\frac{L}{D_3} = \frac{1}{2} \frac{1 - \dfrac{D_{1MF}}{0.3048}}{\cos \beta_{3b}} \qquad (B65)$$

The ratio of mean hydraulic-exit diameter ratio is calculated from the equation

$$\frac{D_{HYD}}{D_3} = \frac{1}{\dfrac{Z_3}{\pi \cos \beta_{3b}} + \dfrac{D_3}{b_3}} + \frac{\dfrac{D_{1T}}{D_3}}{\dfrac{2}{1 - \lambda} + \dfrac{2Z_3}{\pi(1 + \lambda)} \sqrt{1 + \tan^2 \beta_{1T} \left(1 + \dfrac{\lambda^2}{2}\right)}} \qquad (B66)$$

and the ratio of mean relative velocity-impeller exit velocity is determined by

$$\left(\frac{W}{u_3}\right)^2_{av} = \frac{1}{2} \left\{ \left(\frac{V_{m1MF}}{u_3}\right)^2 + \left(\frac{D_{1MF}}{D_3}\right)^2 + \left(\frac{W_3}{W_{1T}}\right)^2 \left[\left(\frac{V_{m1MF}}{u_3}\right)^2 + \left(\frac{D_{1T}}{D_3}\right)^2 \right] \right\} \qquad (B67)$$

Some studies of the effects of the addition of splitter blades on the impeller flow indicated that the mean channel relative velocity is increased in the splitter region. The ratio of mean flow path blade length and hydraulic diameter-exit diameter ratio remain virtually unchanged. Computation of the mean relative velocity ratios for an impeller both with and without splitters showed that, for splitters, the average relative velocity is about 14 percent higher than for conventional impellers. This phenomenon is accounted for by using the constant 7.0 for impellers with splitters and 5.6 for impellers without splitters.

At this point in the iteration procedure the impeller ideal enthalpy rise is calculated as follows:

50

$$\Delta h_{id} = \Delta h_{aero} - \Delta h_{IGV} - \Delta h_{INC} - \Delta h_{SF} - \Delta h_{BL} \tag{B68}$$

Defining the impeller efficiency as

$$\eta_R = \frac{\Delta h_{id}}{\Delta h_{aero}} \tag{B69}$$

the state conditions at the impeller exit are calculated from the relations

$$p'_3 = p'_{2MF} \left(\frac{\eta_R \, \Delta h_{aero}}{C_p T'_0} + 1 \right)^{\gamma/(\gamma-1)} \tag{B70}$$

$$p_3 = \frac{p'_3}{\left(\dfrac{T'_3}{T_3} \right)^{\gamma/(\gamma-1)}} \tag{B71}$$

$$\rho_3 = \frac{p_3}{RT_3} \tag{B72}$$

The value of ρ_3 obtained from equation (B72) is compared to the value estimated in equation (B48).

If the values do not compare within 0.1 percent, the former value is used as a new approximation and equations (B49) to (B72) are iterated until two consecutive values of exit density agree within the tolerance specified.

Recirculation loss. - Recirculation of the working fluid from the vaneless space back into the impeller results in additional work which is lost to the system. Reference 5 expresses this loss as a function of the impeller exit absolute flow angle, impeller diffusion factor, and impeller exit tip speed. The following modified form of the equation of reference 5 is used to calculate the recirculation loss:

$$\Delta h_{RC} = 0.02 \sqrt{\tan \alpha_3} \; D_f^2 u_3^2 \tag{B73}$$

Vaneless diffuser loss. - Reference 7 developed differential equations relating Mach number, flow angle, and total temperature to vaneless diffuser radius ratio through the

51

fundamental relations of continuity, equilibrium, heat transfer, and fluid state. These equations are evaluated at ten equally spaced intervals in the vaneless space. Two iterations of the equations are performed at each station; the first iteration uses the calculated properties at the point of interest to compute the variation in Mach number and flow angle to the next point; the second iteration uses the estimated properties of the downstream point to compute the same variations. The arithmetic average of the two iterations is then used for the solution.

These equations, simplified for adiabatic flow in a geometrically constant depth radial passage are

$$\frac{1}{M^2}\frac{dM^2}{d\overline{R}} = \frac{-2\left(1+\frac{\gamma-1}{2}M^2\right)}{M^2-\sec^2\alpha}\left[(\gamma M^2-\tan^2\alpha)\frac{\zeta}{B\cos\alpha}+\frac{1}{B}\frac{dB}{d\overline{R}}-\frac{\sec^2\alpha}{\overline{R}}\right] \qquad (B74)$$

and

$$\frac{1}{\tan\alpha}\frac{d\tan\alpha}{d\overline{R}} = \frac{\sec^2\alpha}{M^2-\sec^2\alpha}\left\{\left[1+(\gamma-1)M^2\right]\frac{\zeta}{B\cos\alpha}+\frac{1}{B}\frac{dB}{d\overline{R}}-\frac{M^2}{\overline{R}}\right\} \qquad (B75)$$

where

$$\zeta = \frac{C_f r_3}{b_3} \qquad (B76)$$

$$\overline{R} = \frac{r}{r_3} \qquad (B77)$$

$$B = \frac{b}{b_3} \qquad (B78)$$

The schedule of effective passage depth is determined by boundary layer displacement thickness growth on the end walls. The end walls in the vaneless diffuser are assumed to be parallel and have a spacing equal to the impeller exit blade height. The flow pattern between the end walls is approximated as a log spiral between adjacent calculation stations. With these assumptions the incremental flow path length is

$$\Delta S = \frac{r_2 \, \overline{\Delta R}}{\cos \alpha} \qquad \text{(B79)}$$

and the incremental boundary layer displacement thickness is

$$\Delta \delta^* = 0.037 \, S^{-0.2} \left(\frac{V_2}{\nu}\right)^{-0.2} \Delta S \qquad \text{(B80)}$$

where

$$S = \sum_{i=1}^{n} \Delta S_i \qquad \text{(B81)}$$

The effective passage depth is

$$B_{i+1} = B_i - \frac{2 \, \Delta \delta^*}{b_3} \qquad \text{(B82)}$$

and

$$\Delta B = B_i - B_{i+1} \qquad \text{(B83)}$$

Loss the total pressure in the vaneless space is computed from the following equation derived in reference 4:

$$\frac{1}{\left(\dfrac{p_4'}{p_3'}\right)} = 1 + \frac{\gamma C_f}{\cos \alpha_3} \frac{r_3}{b_3} \frac{\displaystyle\int_1^{\overline{R}} M^3 \frac{a}{a'} \frac{\rho}{\rho'} \overline{R} \, d\overline{R}}{M_3 \left(\dfrac{a}{a'}\right)_3 \left(\dfrac{\rho}{\rho'}\right)_3} \qquad \text{(B84)}$$

The integral in equation (B84) is determined by numerical methods. Vaned diffuser leading edge static pressure is calculated from the isentropic relation using the total pressure obtained from equation (B84) and the Mach number obtained from the distribution prescribed by equation (B74)

$$p_4 = \frac{p_4'}{\left(1 + \frac{\gamma - 1}{2} M_4^2\right)^{\gamma/(\gamma-1)}}$$

(B85)

Vaneless diffuser loss is then determined by

$$\Delta h_{VLD} = C_p T_3' \left[\left(\frac{p_4}{p_4'}\right)^{(\gamma-1)/\gamma} - \left(\frac{p_4}{p_3'}\right)^{(\gamma-1)/\gamma} \right]$$

(B86)

Vaned diffuser loss. - Vaned diffuser performance is predicted by use of the test data reported in reference 8. Lines of maximum pressure recovery coefficient at a given area ratio were estimated from the performance maps reported for single plane divergence diffusers with square throats. The component of the vaned diffuser leading edge Mach number parallel to the vane setting angle is used as the throat Mach number. A loss in total pressure associated with this incidence is calculated holding static pressure constant between the leading edge and throat. The throat blockage is estimated from the displacement thickness growth on the vaneless diffuser end walls. Using these conditions of throat Mach number, total pressure, and blockage the pressure recovery of the vaned diffuser is extrapolated for the specified geometric area ratio. Vaned diffuser exit static pressure is then calculated from the relation

$$p_6 = C_p^{**} (p_5' - p_5) + p_5$$

(B87)

The exit total pressure and velocity are determined by trial and error using estimated values of exit critical velocity ratio. The total pressure at the vaned diffuser throat is assumed to be constant across the free-stream area outside the boundary layer displacement thickness. The total pressure and velocity at the vaned diffuser exit are calculated assuming full flow across the geometric area. Starting with a low value of $\left(V/V_{cr}\right)_6$ the lower estimate of exit total pressure is expressed as

$$p_6' = \frac{p_6}{\left[1 - \frac{\gamma - 1}{\gamma + 1} \left(\frac{V}{V_{cr}}\right)_6^2\right]^{\gamma/(\gamma-1)}}$$

(B88)

and the higher estimate is

$$p_6' = \frac{\left(\dfrac{\rho V}{\rho' V_{cr}}\right)_5 p_5'}{AR \left(\dfrac{\rho V}{\rho' V_{cr}}\right)_6} \tag{B89}$$

where

$$\left(\frac{\rho V}{\rho' V_{cr}}\right)_5 = \frac{w}{\rho_5' \left(V_{cr}\right)_5 A_5 B_5} \tag{B90}$$

Equations (B88) and (B89) are solved using increasing values of $\left(V/V_{cr}\right)_6$ until convergence is achieved. The vaned diffuser loss is then calculated from the relation

$$\Delta h_{VD} = C_p T_3' \left[\left(\frac{p_6}{p_6'}\right)^{(\gamma-1)/\gamma} - \left(\frac{p_6}{p_5'}\right)^{(\gamma-1)/\gamma} \right] \tag{B91}$$

Efficiency decrements. - Decrements in efficiency caused by the individual losses are obtained from the following equations:

$$\Delta \eta_{IGV} = \frac{\Delta h_{IGV}}{\Delta h_{act}} \tag{B92}$$

$$\Delta \eta_{INC} = \frac{\Delta h_{INC}}{\Delta h_{act}} \tag{B93}$$

$$\Delta \eta_{BL} = \frac{\Delta h_{BL}}{\Delta h_{act}} \tag{B94}$$

$$\Delta \eta_{SF} = \frac{\Delta h_{SF}}{\Delta h_{act}} \tag{B95}$$

55

$$\Delta h_{DF} = \frac{\Delta h_{DF}}{\Delta h_{act}} \tag{B96}$$

$$\Delta \eta_{RC} = \frac{\Delta h_{RC}}{\Delta h_{act}} \tag{B97}$$

$$\Delta \eta_{VLD} = \frac{\Delta h_{VLD}}{\Delta h_{act}} \tag{B98}$$

$$\Delta \eta_{VD} = \frac{\Delta h_{VD}}{\Delta h_{act}} \tag{B99}$$

where

$$\Delta h_{act} = \Delta h_{aero} + \Delta h_{RC} + \Delta h_{DF} \tag{B100}$$

Overall efficiency. - The overall total efficiency is calculated as follows:

$$\eta_{AD} = \frac{\Delta h_{aero} - (\Delta h_{IGV} + \Delta h_{INC} + \Delta h_{BL} + \Delta h_{SF} + \Delta h_{VLD} + \Delta h_{VD})}{\Delta h_{aero} + \Delta h_{RC} + \Delta h_{DF}} \tag{B101}$$

56

REFERENCES

1. Galvas, Michael R.: Analytical Correlation of Centrifugal Compressor Design Geometry for Maximum Efficiency With Specific Speed. NASA TN D-6729, 1972.

2. Stewart, Warner L.; Whitney, Warren J.; and Wong, Robert Y.: A Study of Boundary-Layer Characteristics of Turbomachine Blade Rows and Their Relation to Over-All Blade Loss. J. Basic Eng., vol. 82, no. 3, Sept. 1960, pp. 588-592.

3. Rohlik, Harold E.: Analyitical Determination of Radial Inflow Turbine Design Geometry for Maximum Efficiency. NASA TN D-4384, 1968.

4. Stanitz, John D.: Effect of Blade-Thickness Taper on Axial-Velocity Distribution at the Leading Edge of an Entrance Rotor Blade Row With Axial Inlet, and the Influence of This Distribution on Alinement of the Rotor Blade for Zero Angle of Attack. NACA TN-2986, 1953.

5. Coppage, J. E.; Dallenbach, F.: Eichenberger, J. P.; Hlavaka, G. E.; Knoernschild, E. M.; and Vanke, N.: Study of Supersonic Radial Compressors for Refrigeration and Pressurization Systems. AiResearch Mfg. Co. (WADC TR-55-257), Dec. 1956.

6. Shepherd, Dennis G.: Principles of Turbomachinery. Macmillan Co., 1956.

7. Stanitz, John D.: One-Dimensional Compressible Flow in Vaneless Diffusers of Radial- and Mixed-Flow Centrifugal Compressors, Including Effects of Friction, Heat Transfer, and Area Change. NACA TN 2610, 1952.

8. Runstadtler, Peter W., Jr.: Pressure Recovery Performance of Straight-Channel, Single-Plane Divergence Diffusers High Mach Numbers. Rep. N-88, Creare, Inc. (USAAVLABS-TR-69-56, AD-865300), Oct. 1969.

9. Rodgers, Colin: Typical Performance Characteristics of Gas Turbine Radial Compressors. Paper 63-AHGT-14, ASME, Mar. 1963.

10. Stewart, Warner L.: Analytical Investigation of Flow Through a High-Speed Mixed-Flow Turbine. NACA TM E51H06, 1951.

11. Weisner, F. J.: A Review of Slip Factors for Centrifugal Impellers. J. Eng. Power, vol. 89, no. 4, Oct. 1967, pp. 558-572.